1-1-2006

Multiscale Structure-Function Relations of a Tendon

Lakiesha Nicole Williams

MULTISCALE STRUCTURE-FUNCTION RELATIONS OF A TENDON

By

Lakiesha Nicole Williams

A Dissertation
Submitted to the Faculty of
Mississippi State University
in Partial Fulfillment of the Requirements
for the Degree of Doctorate of Philosophy
in Biomedical Engineering
in the Department of Agriculture and Biological Engineering

Mississippi State, Mississippi

August 2006

MULTISCALE STRUCTURE-FUNCTION RELATIONS OF A TENDON

By

Lakiesha Williams

Approved:

_____ Steven H. Elder, PhD Associate Professor in Biomedical Engineering Graduate Coordinator of the Department of Biomedical Engineering (Major Advisor and Director of Thesis)	_____ Mark F. Horstemeyer, PhD Center for Advanced Vehicular Department Systems Chair Computational Solid Mechanics Professor of Mechanical Engineering (Minor Advisor and Committee Member)
_____ Joseph A. Chromiak, PhD Associate Professor – Kinesiology Interim Department Head of Kinesiology (Committee Member)	_____ Jerome A. Gilbert, PhD Associate Provost and Associate Vice President for Academic Affairs (Committee Member)
_____ Ronald McLaughlin, D.V.M., D.V.Sc., A.C.V.S. Associate Professor Mississippi State University College of Veterinary Medicine Department of Clinical Sciences (Committee Member)	_____ Kirk H. Schultz, PhD Dean of the College of Engineering

Name: Lakiesha Nicole. Williams

Date of Degree: August 5, 2006

Institution: Mississippi State University

Major Field: Biomedical Engineering

Major Professor: Dr. Steven H. Elder

Title of Study: MULTISCALE STRUCTURE-FUNCTION RELATIONS OF A TENDON

Pages in Study: 118

Candidate for Doctor of Philosophy Degree

In 1998, the United States National Committee on Biomechanics (USNCB) established an evolving discipline called Functional Tissue Engineering (FTE). In establishing this discipline, the goals of the USNCB were to advance FTE by increasing awareness among tissue engineers about the importance of restoring function when engineering tissue constructs. Another goal was to encourage tissue engineers to incorporate these functional criteria in the design, manufacturing and optimization of tissue engineered constructs. Based on this motivation, an investigation of the structure and mechanical properties of the rabbit patellar tendon was executed, with the ultimate goal of creating a multiscale soft tissue model based on internal state variable (ISV) theory. Many continuum scale models, mostly phenomenological and microstrucutral, have been created to contribute to the understanding of the complex functional

properties of the tendon, such as its anisotropy, inhomogeneity, nonlinearity, and viscoelasticity. However, none of these models have represented the mechanical behavior of the tendon in the presence of internal structural change on a multiscale level. The development of a multiscale ISV model will allow the capture of the irreversible, path history dependent aspects of the material behavior. The objective of this study is to contribute to the multiscale ISV model development by quantifying the structure-function relations of tendons. In particular, the fibril distribution at the microstructural level and the resultant multiaxial stress states (longitudinal and transverse compression and longitudinal tension) was examined.

DEDICATION

I would like to dedicate this dissertation to the many family and friends that have supported me throughout this long journey. Specifically, I would like to express my love and gratitude to my mother Deborah Claude, and sisters Rochshall Claude and Trimica Belle for their encouragement and support. Extreme thanks and much love goes out to my best friend and husband, Mr. Byron J. Williams, for constantly encouraging me and diligently laboring alongside of me on my road to completion. It has been a wonderful experience. Last, but not least I would like to dedicate this work to one of my biggest supporters, my wonderful father, the late Rodney J. Claude.

ACKNOWLEDGEMENTS

It has been a long journey to the Ph.D. and I would need to write another dissertation to acknowledge all of those who have played a role in my life as I have been on this road to completion. First, I would like to acknowledge and thank my major advisor, Dr. Steven H. Elder, who appears to be a miracle worker. His hands-on approach showed me that I could make anything work with some innovation. Thanks to my minor advisor, Dr. Mark Horstemeyer, for his mentorship, advice, and for introducing me to and guiding me through the complexity of modeling. Dr. Jerome Gilbert is greatly acknowledged for being a great support as both my former department head and committee member. Dr. Ronald McLaughlin is to be thanked for being on my committee and assisting with the small animal surgeries. Great appreciation goes out to Dr. Joseph Chromiak for his input and for being on my committee. I would like to acknowledge Dr. William Batchelor and the Agricultural and Biological Engineering department for both helping and encouraging me to finish. Thanks to Srikanth Subramanian for assisting me with the testing and experiments. Also, thanks to the Center for Advance Vehicular systems for the great workspace and for assisting me in my career and professional development. Great appreciation

goes to Bill Monroe and Amanda Lawrence at the Electron microscopy center. Gratitude is extended to Marybeth Lima for being a mentor and supporting me since I began college. Thanks to my husband Byron for helping run the last set of gruesome tension tests. I don't know if I could have completed the tests without him.

Last, but certainly not least, I would like to give all praise and honor to my personal Lord and Savior, Jesus Christ. It has been by my faith in Jesus and the gifts that He has given me that has enabled me to believe that I could do anything. I thank God for loving me so much that He would choose me to begin such a task and give me the wisdom and grace to complete it. The real credit goes to my Lord who has equipped me for this predestined purpose. He has definitely worked through me to accomplish the, sometimes seemingly impossible, Ph.D. and because of His love I know that the best is yet to come. Thank You Lord!!!

TABLE OF CONTENTS

LIST OF TABLES

LIST OF FIGURES

FIGURE Page

FIGURE Page

FIGURE Page

CHAPTER I

INTRODUCTION

Model Motivation

The mechanical role of soft skeletal connective tissues is very important. In observing the challenges that tissue engineers face in repairing and replacing tissues that serve a predominantly biomechanical function, the United States National Committee on Biomechanics (USNCB) established an evolving discipline called Functional Tissue Engineering (FTE). The goals of the USNCB in advancing FTE are to: (1) Increase awareness among tissue engineers about the importance of restoring "function" when engineering tissue constructs, (2) Identify the critical structural and mechanical requirements needed for each tissue engineered construct, and (3) encourage tissue engineers to incorporate these functional criteria in the design, manufacturing and optimization of tissue engineered constructs (Butler et al. 2000).

Several principles were put in place for FTE by the USNCB. If followed correctly, these principles could dramatically influence the quality of the design of soft tissue implants. Also, the results could assist in model development, which could be implemented into Finite Element Analysis software for

accurate simulations of soft tissue. These principles are (1) measure *in vivo* Stress and Strain Histories in normal tissues for a variety of activities, (2) establish mechanical properties of the native tissues for sub-failure and failure conditions, (3) select and prioritize a subset of these mechanical properties, (4) Set standards when evaluating repairs/replacements after surgery to determine "How Good is Good Enough?", (5) determine the physical regulations that cells may experience *in vivo* as they interact with the extracellular matrix, and (6) Determine if cell-matrix implants can be stimulated before surgery to produce a better outcome. Due to the complex nature of biological materials, the fundamental understanding of the structure-property relations is in its infancy. Some of the complex structural and functional properties that remain unclear are anisotropy, geometry, inhomogeneity, nonlinearality, and viscoelasticity.

Establishing a sound understanding of the material properties in soft tissue is important as they can be used in the prediction of mechanical response of the tissue. Understanding these properties also will enable more effective development in the design and manufacturing of tissue engineered constructs (An 2005). Numerous models have been established to determine the mechanical properties and evaluate the complex nature of soft skeletal connective tissues with the main purpose being to enhance the understanding of the fundamental bases of the material. These soft tissue continuum scale models can be grouped into two major categories: microstructural and phenomenological. As in its name, the purpose of the microstructural model is to

capture the detailed mechanical responses of the internal (micro) structures of the materials. The responses of these constituents are combined to produce a description of the material. Characteristic microstructural models evaluate the uncrimping and stretching of fibers and possibly take into account the number of fibers within the tissue, the fiber diameter distributions and the area fraction of fibers (Wren et al. 1998). Phenomenological models, also known as rheological models, attempt to describe the gross mechanical response of the material by simplifying the structure of the tissue. They describe the material's behavior, but do not relate the behavior explicitly to the tissue structure or components (Weiss et al. 2001). Classic phenomenological models describe the tissue as a mixture of two phases: a fluid and a solid (Setton et al. 1992; Ateshian et al. 1997; Yin et al. 2004). The viscoelastic response of rheological tissue models are often represented with a series of springs and dashpots. Continuum models are full scale models of the tissue based on its direct response to stresses and strains (Johnson et al. 1996; Pioletti et al. 1998). Continuum models may assist in understanding the natural tissue responses while subjected to complex loads, however, the changing internal structure may or may not be incorporated into the model. Microstructural and phenomenological models are usually developed to approximate an overall continuum response.

Some models were developed using the phenomenological approach by using mechanical constructs such as springs and dashpots, continuum formulations, or quasi-linear viscoelasticity theory (Wren et al. 1998). Although

they are phenomenologically sufficient in explaining the constitutive behavior of the soft tissue, they do not explain the structure-property relationships within the model; therefore, the underlying behavior of the material remains unknown. Wren et al. (1998) developed a phenomenological based model; however, the authors assumed tissue homogeneity, isotropy and no time dependent effects. Therefore, the overall phenomenon of the model was not representative of real tissue. Yin and Elliot (2004) developed a biphasic and transversely isotropic mechanical model for rat tail tendons without regard to the tissue constituents. Their results were effective in correlating fluid flow to viscoelasticity. However, they did not consider the configuration of fibrils (area fraction, number density) in their fluid flow model, which would have an effect on fluid flow due to the macromolecules attached to fibrils.

Microstructural models also have been formulated to examine the uniaxial tensile behavior of parallel fibered soft tissues. Many of these structural models have not taken into consideration the importance of the volumetric fraction of the fibers on the mechanical properties of the material by evaluating structural-function relations (Woo 1982; Yamamoto et al. 1992). Wren et al. (1998) considered the volumetric fraction of fibrils within the material as they modeled the constitutive and failure behavior of soft connective tissues; however, just as numerous other models, the multiple hierarchical levels of the tendon were not considered.

Along with limited microstructual representation in models, the models demonstrate a lack of ability to accurately predict responses to load, referred to as stress state dependency. In their development of a constitutive model of the time dependent and cyclic loading of elastomers, Bergstrom et al. (2001), closely predicted strain rate and hysteresis of some soft tissues (Bergstrom et al. 2001). They also included the kinetics or the flow behavior of the tissue; however, they did not include stress state dependency in the model. Unlike Bergstom's model, many other constitutive models for soft tissue are single integral models; therefore, they only examine the average effects of change in the material and not the internal structural changes at every moment in time. The scientific literature has not shown the existence of a general purpose model for viscoelastic soft tissues, which covers a broad range of effects such as the effect of variations in volumetric fractions, variations in strain rates, and stress state dependence. Therefore, it is the objective of this study to contribute to the development of a next generation multiscale model by quantifying the structure-function relations of the rabbit patellar tendon and provide input for the model. In particular, the fibril distribution at the microstructural level and the resultant multiaxial stress states (longitudinal and transverse compression and longitudinal tension) will be examined.

Internal State Variable Constitutive Theory

Internal state variable (ISV) constitutive models, which are based on a thermodynamic framework, have been constructed to analyze the irreversible,

path dependent aspects of material behavior. ISVs are differential variables and are functions of observable, variables such as temperature and stress state (Coleman et al. 1967). Internal variables also are known as hidden variables because they are “hidden” or “internal” to the material and represent microstructure, defects, grains, etc. The highly irreversible properties of soft tissues allow it to be a candidate in which ISVs could be applied. The irreversible components of a viscoelastic material are primarily due to the viscous nature of soft tissue. Due to viscosity, energy is dissipated in the structure and ultimately inelastic behavior results and causes irreversibility of mechanical properties.

ISV applications have been extensively studied in solid mechanics; however, the presence of ISVs applied to soft tissue is limited. An internal state variable was included in the development of a three dimensional non linear model for dissipative response to soft tissue (Rubin et al. 2002). The state variable was used in the constitutive formulations of both superficial musculoaponeurotic system (SMAS) and skin. Hardening was used as a state variable in this formulation and it was used to model the effective hardening associated with fluid flow through the cells of the tissue. The authors observed hardening due to the loss of fluid during loading and dissipation, as well as recovery to re-absorption of fluid. This model was successful in its prediction of stress-relaxation phenomena. However, additional microstructural information should be included in the functional forms of the evolution equations for detailed modeling of the tissues, specifically, the authors should include information on

fiber size and distribution in the tissues. Wei et al. (2003) developed a constitutive model of a polymeric material using ISVs. High Density Polyethylene (HDPE) was used for the model and results demonstrated that their constitutive model was more flexible for describing the strain rate sensitivity of polymeric materials over a wide range of strain rates. However, the model did not include path history dependency or microstructural details.

Onat et al (1988) demonstrated that tensorial ISVs constitute a natural tool for the representation of internal structure and its orientation. ISVs also provide a convenient measure of the degree of anisotropy present in the material. Studies have shown that representations based on the notion of state and on the differential equations that govern the evolution of state have definite advantages over other methods of representation (i.e. integral representation). Some examples of the application of ISVs in metals are hysteresis due to plastic deformation or phase transition and fatigue and fracture (McDowell 2005). McDowell also noted that some of these processes occur so slowly and so near equilibrium that common models forego description of nonequilibrium aspects of dissipation (e.g. grain growth). Just as in metals, it is also known that defects that occur in soft tissue occur at the nanoscale, where the decorin glycosaminoglycans (GAGS) bridge with adjacent fibrils. This damage may lead to macroscale damage and eventually failure (Redaelli et al. 2003). This phenomenon has been studied computationally; however, there are no models that consider the nanoscale of damage. ISV constitutive theory offers an in-depth

basis for incorporating irreversible, path dependent behavior that can be informed by experiments, computational materials science and micromechanics (McDowell 2005). One pure advantage of an ISV model is the ability to alleviate boundary conditions when instituting the model in a finite element (FE) environment. This asset is due to the model's ability to predict path history dependence and complex boundary value problems.

Soft tissue ISV formulations have not been thoroughly applied in research; therefore, the development of an internal state variable formulation will be based on the examination of the parameters used for the development of an aluminum ISV formulation. In an examination of an A356 aluminum alloy, Horstemeyer (2001) showed that the model development must account for microstructure/inclusion sizes, distributions and nearest neighbor distances. The goal of the ISV model was to develop the ability to predict damage progression in the aluminum alloy. Cocks and Ashby (1982) showed that the progression of damage in almost all ductile materials subjected to monotonic loading is due to void nuclueation (initiation of pores), void growth (growth of pores) and void coalescence (merging of pores) within the material substructure. Due to its heterogeneous microstucture, cast alumninum alloys are even more prone to these types of damage progressions. Damage in this material can be quantified as the ratio of the change in volume of an element. This formulation is based on the void nucleation density and void growth. The area fraction, growth and number density of voids will significantly impact the damage progression of the

aluminum alloy. The particles which exist at the microstructural level also contribute to the mechanical integrity of the material and their area fractions and number densities should be quantified.

As obvious, this classification of damage may not directly apply to that of the tendon considering that the tendon is not metallic in nature. However, the underlying concept of damage relating to volumetric changes will be considered when developing the ISV model for the tendon. For example, soft tissue internal state variable formulations should be synonymous to the major damage components in metals which are (1) the hardening equations (kinematic and isotropic hardening), (2) the time dependent elasticity equations, and (3) void nucleation, void growth, and void coalescence. Therefore, before specifically quantifying damage parameters of the rabbit patellar tendon, it is our focus to define the functions of the tissue that affect the underlying microstructure. We are developing an experimental database of which we could later determine the mathematical responses. This dissertation will focus on exploratory examinations of the area fractions, number density and diameter distributions of the fibrils in the tendon. We are examining the fibers because it has been shown that force is transferred through the nanometer sized fibers and therefore, they are known to play a key role in force output. Although not included in this study, exploratory studies of proteoglycans (PGs) and glycosaminoglycans (GAGs) and their relation to force output along with studies of polymer fiber distortion should be included to demonstrate the magnitude in which these functions affect the

tissue's underlying microstructure. After a complete understanding of the role of the underlying microstructure the soft tissue formulations of the ISV equations will be developed.

The major principles that this dissertation will focus on are the establishment of mechanical properties of the rabbit patellar tendon for sub-failure conditions along with structural evaluation of the native tissues for the development of a multiscale ISV model. In order to develop the multiscale ISV model, detailed experimental data from nanoscale to micronscale, mesoscale, and microscale should be available. Upon collecting the necessary data via experimentation, it is then possible to bridge length scales and quantify the relationships between the microstructure and mechanical properties. The major mode of testing for tendons is continuum scale tension loading (Woo 1982; Yamamoto et al. 1992; Danto et al. 1993; Johnson et al. 1994; Yamamoto et al. 1998). This is primarily due to the fibers being oriented along the tensile axis and tension being the tendon's main functioning mode. Due to this cause, it is imperative that more tests are performed to assist in the development of a multiscale, multistress state ISV model. Table 2.1 shows a list of the test data that is currently accessible and available for use. The *"NOT"* denotes limited to no availability and the *"A"* denotes availability. This study will include exploratory tests for input into the model.

Table 1.1

Availability of rabbit patellar tendon data at various size scales

	TENDON		FASCICLE		FIBRIL	
	Longitudinal	Trans-verse	Longitudinal	Trans-verse	Longitudinal	Trans-verse
TENSION	A (Yamamoto et al. 1992)	A (Yamamoto et. al, 2000)	NOT (Yamamoto et al. 1999)	NOT	NOT	NOT
COMPRESSION	NOT	NOT	NOT	NOT	NOT	NOT
SIMPLE SHEAR	A Our group	A Our group	NOT	NOT	NOT	NOT
INDENTER	n/a	NOT	NOT	NOT	NOT	NOT
VOLUMETRIC FRACTION	n/a		NOT		NOT	
Key:	A denotes Availability				NOT denotes limited to No Availability	

Three separate studies were performed to contribute to model development. In study 1, examined the structure of the tendon in five locations on the tissue were examined. The five locations were the central center, central proximal, central distal, medial center, and lateral distal sections. The purposes of this investigation were to provide microstructural information on the rabbit patellar tendon for input into the multiscale model and to compare microstructural information among various regions of the rabbit patellar tendon. The rabbits

were euthanized and the patellar tendon resected from the rabbit. The tendons were placed in fixative and prepared for Transmission Electron Microscopy (TEM). After TEM processing, electron micrographs of 14 equal sized fibril fields within the fascicles of each tendon segment were obtained (20,000 X magnification). The image areas were 6.4 x 4.3 μ^2 with number of fibrils per image ranging from 242 to 1055. The images were digitized and the number density, area fraction, and diameter distributions were determined from each image. A Univariate ANOVA method was used to determine statistical significance of mean fibril diameter based on location within the tendon.

In study 2, compression testing was performed on the rabbit patellar tendon in both the longitudinal and transverse directions. The purpose of this investigation was to contribute to the understanding of the longitudinal and transverse mechanical properties of tendons under compressive loads, with the final goal of using this data to develop a multiscale, viscoelastic model that accounts for multiple stress states (tension, compression, simple shear). This compression data contributed to the development of the transverse and longitudinal Von Mises stress-strain responses that illustrated the compressive anisotropy of the tendon. Five methods of compression were performed in order to examine the variation in mechanical responses. Three methods of compression were examined in the longitudinal direction and two methods of compression within the axial direction. The tendons were compressed transverse (n=11) to the fiber direction and along the fiber direction (n=16). In

preparation for each test, the thickness of each sample was measured using the Mach-1^{TM} (Biosyntech Inc., Canada) micro mechanics testing machine. The Mach-1^{TM} micromechanical testing machine also was used to apply compression for each method. Experimental setup slightly varied between each method. The primary differences in the setup was the changing of platens and the cyanoacrylate used for longitudinal compression tests. The experimental environment was in an incubator at 37 ºC, 5% carbon Dioxide gas. The protocols were constant for all five of the methods.

In study 3, the structure-function relationships of the tendon were evaluated by subjecting the tissue to tensile loading and gathering microstructural information based on percent strain. Changes in microstructure were evaluated for the tendon at 3%, 4% and 6% strain. Whole patellar tendons underwent tension testing on an MTS 858 (MTS, Eden Prairie, MN) mechanical testing machine. In preparation for mechanical testing, both the muscle and fat tissue were completely removed from the tibia and the fat tissue removed from the tendon. Prior to potting the tibia in an acrylic resin (Jorgensen Laboratories, Loveland, CO.), the tibia was cut to a desired length. A customized fixture was used to grip the patellar bone and a 2500 kg load cell was used to apply the axial load to the tendon. After potting and gripping the tendon, two dark lines were applied to the tendon by attaching monofilament nylon suture to the tendon with cyanoacrylate. A Visual Dimension Analyzer (VDA) (Living Systems Instrumentation, Burlington, VT) was used to measure the visual change in strain

between the dark lines. The center portion of the sutures was set as a diameter measurement on the VDA system. Individually, as the tendons were pulled and as the diameter measurement increased to 3%, 4%, or 6% of its initial measurement, the tests were held at the constant strain. While being held at their respective percent strains, the specimens were injected with 10 cc's of fixative solution (5 cc's given at 10 minute intervals for 20 minutes). The tendons were then detached with a scalpel, and the central center piece dissected and placed at 4ºC in a vial of fixative (½ strength Karnovsky's (in 0.1M cacodylate buffer -pH 7.2) in preparation for TEM. While being tested, the tendons were continuously sprayed with a saline solution to retain moisture. Load, displacement, and VDA data was recorded via a local computer. The control samples were attached to the MTS system, a preload of 1.5 kg was applied and the monofilament sutures placed on the tendon. The TEM process used in study 1 was replicated for these samples and one sample was analyzed for each treatment (control, 3%, 4% and 6% strain).

The long term objective of this research is to develop a multiscale, Internal State Variable (ISV), viscoelastic material model that is validated by multiaxial experiments on the rabbit patellar tendon. For this study, multiaxial refers to uniaxial tension, compression, and simple shear. In order to develop the various aspects of the model, preliminary information is required and this project will provide aspects of that preliminary information.

Research Question

Can the structural property relations of the rabbit patellar tendon be determined?

Research Motivation

Does a general purpose model exist, for soft tissue that covers accurately, a broad range of effects, including history effects, which includes high fidelity physics?

References

[1] An KN (2005) Role of biomechanics in functional tissue engineering. In:Mechanical properties of bioinspires and biological materials. (ed) Viney C, Katti K, Ulm FJ and Hellmich C. Materials Research Society, Warrendale

[2] Ateshian GA, Warden WH, Kim JJ, Grelsamer RP and Mow VC (1997) Finite deformation biphasic material properties of bovine articular cartilage from confined compression experiments. Journal of Biomechanics 30:1157-1164

[3] Bergstrom J and Boyce M (2001) Constitutive modeling of the time-dependent and cyclic loading of elastomers and application to soft biological tissues. Mechanics of Materials 33:523-530

[4] Butler D, Goldstein S and Guilak F (2000) Functional tissue engineering: The role of biomechanics. Journal of Biomechanics 122:570-575

[5] Cocks A and Ashby M (1982) On creep fracture by void growth. Progress in Materials Science 27:189-244

[6] Coleman B and Gurtin M (1967) Thermodynamics with internal state variables. The Journal of Chemical Physics 47:597-613

[7] Danto M and Woo S (1993) The mechanical properties of skeletally mature rabbit anterior cruciate ligament and patellar tendon over a range of strain rates. Journal of Orthopedic Research 11:58-67

[8] Horstemeyer M (2001). From atoms to autos. A new design paradigm using microstructure-property modeling: Monotonic loading conditions. Albuquerque, Sandia National Laboratories.

[9] Johnson G, Tramaglini D, Levine R, Ohno K, Choi N and Woo S (1994) Tensile and viscoelastic properties of human patellar tendon. Journal of Orthopedic Research 12:796-803

[10] Johnson G, Livesay G, Woo S and Rajagopal K (1996) A single integral finite strain viscoelastic model of ligaments and tendons. Journal of Biomechanical Engineering, 118:221-226

[11] McDowell D (2005) Internal State Variable Theory. In:Handbook for materials modeling. (ed) Yip S. Springer, The Netherlands

[12] Onat E and Leckie F (1988) Representation of mechanical behavior in the presence of changing internal structure. Journal of Applied Mechanics 55:1-10

[13] Pioletti D, Rakotomanana L, Benvenuti J and Leyvraz P (1998) Viscoelastic constitutive law in large deformations: application to human knee ligaments and tendons. Journal Biomechanics 31:753-757

[14] Redaelli A, Vesentini S, Soncini, M, Vena P, Mantero S and Montevecchi F (2003) Possible role of decorin glycosaminoglycans in fibril to fibril force transfer in relative mature tendons – a computational study form molecular to microstructural level. Journal of Biomechanics 36:1555-1569

[15] Rubin M and Bodner S (2002) A three-dimensional nonlinear model for dissipative response of soft tissue. International Journal of Solids and Structures 39:5081-5099

[16] Setton LA and Mow VC (1992) A generalized biphasic poroviscoelastic model for articular cartilage: Theory and experiements. American Society of Mechanical Engineers, Bioengineering Division (Publication) BED 22:589-592

[17] Wei P and Chen J (2003) A viscoelastic constitutive model with nonlinear evolutionary internal variables. Acta Mechanica 164:217-225

[18] Weiss J and Gardiner J (2001) Computational modeling of ligament mechanics. Critical Reviews in Biomedical Engineering 29:303-371

[19] Woo SL (1982) Mechanical properties of tendons and ligaments. Biorheology 19:385-396

[20] Wren T and Carter D (1998) A microstructural model for the tensile constitutive and failure behavior of soft skeletal connective tissues. Journal of Biomechanical Engineering 120:55-61

[21] Yamamoto E , Hayashi K, Kuriyama H, Ohno K, Yasuda K and Kaneda K (1992) Mechanical properties of the rabbit patellar tendon. Journal of Biomechanical Engineering 114:332-337

[22] Yamamoto N and Hayashi K (1998) Mechanical properties of rabbit patellar tendon at high strain rate. Bio-Medical Materials and Engineering 8:83-90

[23] Yin L and Elliott D (2004) A biphasic and transversely isotropic mechanical model for tendon: Application to mouse tail fascicles in uniaxial tension. Journal of Biomechanics 37:907-91

CHAPTER II

VARIATION OF DIAMETER DISTRIBUTION, NUMBER DENSITY, AND AREA FRACTION WITHIN FIVE AREAS OF THE RABBIT PATELLAR TENDON

Abstract

The purposes of this investigation are to provide microstructure information on the rabbit patellar tendon for input into a multiscale model and to compare microstructural information at various regions of a rabbit patellar tendon. The properties of the rabbit patellar tendon are well documented mechanically, but detailed microscopy information is not available. Microstructural examination of the tendon fibrils is for understanding the structure function relations within the tissue. Limited microscopy studies on rabbit patellar tendon collagen fibrils have been computed. Furthermore, evaluation of structure-function relations in multiple regions of any one of the same tissue type have not been conducted. In this study the number density, area fractions, and diameter distributions of fibrils were determined. In grouping sections, based on their locations, the results showed a statistically significant difference of the tendon structure between the center and proximal locations. Also, the central region showed bimodality in fibril distribution.

Introduction

The tendon, essentially a uniaxial composite material, is a soft viscoelastic tissue whose anatomical structure connects muscle to bone. Its major purpose is to transmit the force created in muscle to bone and make joint movement possible (Kannus 2000). The tendon is composed of a complex structural make-up. Its primary composition is collagen fibrils within a matrix, but many of the components within the tendon contribute to its mechanical behavior. This detailed structural make-up consists of mostly type I collagen fibrils (65-80% dry weight) and elastin (1-2% dry weight) arranged into bundles collectively with fibroblasts and proteoglycans (Kannus 2000). The tendon, which uses collagen as the major load-bearing constituent, has a hierarchical structural architecture. Ligaments and tendons have been described as a nested hierarchy of cross-linked micro-fibrils, fibrils, and fiber bundles (or fascicles) (Kastelic et al. 1978). Figure 2.1 shows this structural hierarchy, which begins with collagen at the molecular level, proceeds to fibrils (nanometer scale), fascicles (micron scale), and the whole tendon (macro scale). The sub fibrils are arranged in such a manner in that they lie individually in the shallow recesses of the tendon cell surface. As the length scale increases, the sub fibrils become aggregated into fiber bundles or fibrils. The fiber bundles are separated from other fiber bundles throughout the tendon by tendon cells only. A collection of these fiber bundles, which are called fascicles, are surrounded by loose areolar tissue called

endotenon. The tendon is a multi-fasclicled structure and is surrounded by a sheath that encloses the whole structure called the epitenon.

Along with the complex hierarchical arrangement, collagen fibers within the tendon also display a crimping pattern. This pattern is a universal phenomena that is exhibited in the tendons of all animals as well as within numerous other collagenous tissues that are subjected to tensile loading in other organisms (Kastelic et al. 1978). Within the early stages of deformation uncrimping occurs, which gives rise to the initial toe region in the stress-strain curve.

In evaluating the mechanical properties of a material it is also important to examine the structural relations, in particular, the microstructural properties. Mechanics in the tendon are known to also occur at the nanoscale level. For example, Redaelli observed that the macromolecules, glycosaminoglycan (GAGs), bound to decorin, serve as bridges between contiguous fibrils, connecting adjacent fibrils every 64-68 nanometers (Kastelic et al. 1978). As the GAGs are bound to the tendon they play a role in stress transfer through the fibrils to the whole tendon, which makes them intricately involved in the mechanical integrity of the tissue. Since the GAGS are attached to fibrils, GAG breakdown or damage will effect fibril force output and, in turn, have a significant effect on macroscale force production, which may limit the effectiveness of the tissue. Mechanical and microscopic evaluation at lower structural scales within the tendon may provide insight into macroscopic damage/failure mechanisms.

Although previous studies have provided insight on the mechanics and structure of the tendon at the macroscale level (Yamamoto et al. 1992; Sasaki et al. 1996; Toyhama et al. 2002), limited information has been rendered from the lower length scales of structure-function relationships. The importance of structure-function relationships was evaluated by Atkinson et al (1999) as various cross sectional sizes of the tendon were obtained and their stress relaxation showed variations based on the cross sectional area. Their results showed that the smaller (~1mm^2) specimens exhibited a higher tensile modulus, a slower rate of relaxation, and a lower amount of relaxation in comparison to larger specimens (~20mm^2) from the same location in the same tendon. Based on their results, the authors concluded that underlying structures probably influence the mechanical behavior of the tendon. Derwin et al (1999) also investigated the structure-property relationships in a tendon fascicle model and reported a positive correlation between mean fibril diameter and fascicle stiffness and maximum load. If fibril sizes vary within a tendon, there may be a gradient of stress throughout the tendon and other variations in mechanical responses.

No specific structural data is published based on the various areas within the tendon (e.g. central center, central proximal, central center, central proximal, central distal, and lateral distal). Sklenka et al. (2006) recently published a study on the effect of fibril diameter in rabbit patellar tendon repair. Their study included microscopic examinations of the patellar-end, middle, and tibial-end of the patellar-tendon complex. They indicated that sample location had a

significant effect on collagen fibril diameter between the experimental and control subjects. The mean fibril diameters of the middle section of the tendon were consistently greater than that of the proximal and distal sections.

The overall objective of this study is to quantify the structures of a tendon and to incorporate the results into an internal state multiscale model. Many of the continuum models developed in the past describe the material behavior, but do not relate the behavior explicitly to the tissue structure or components (Setton et al. 1992; Ateshian et al. 1997; Yin et al. 2004). The literature has not shown the existence of a general purpose model for viscoelastic soft tissues, which covers a broad range of effects such as variations in volumetric fractions, variations in strain rates, and other stress state dependency. The purposes of this investigation were: (1) to provide microstructure information on the rabbit patellar tendon, a tissue that is well documented mechanically, but does not have detailed microscopy information available, and (2) to provide microstructural information within six regions of the tendon. Specifically, fibril data from the central center, central proximal, central distal, medial center and lateral distal areas of the tendon were collected and the differences between their area fractions, number density, and diameter distributions were examined based on their location in the tendon. The rabbit patellar tendon model was implemented due to its large size and accessibility (the tendons were retrieved from rabbits used for a separate and unrelated study).

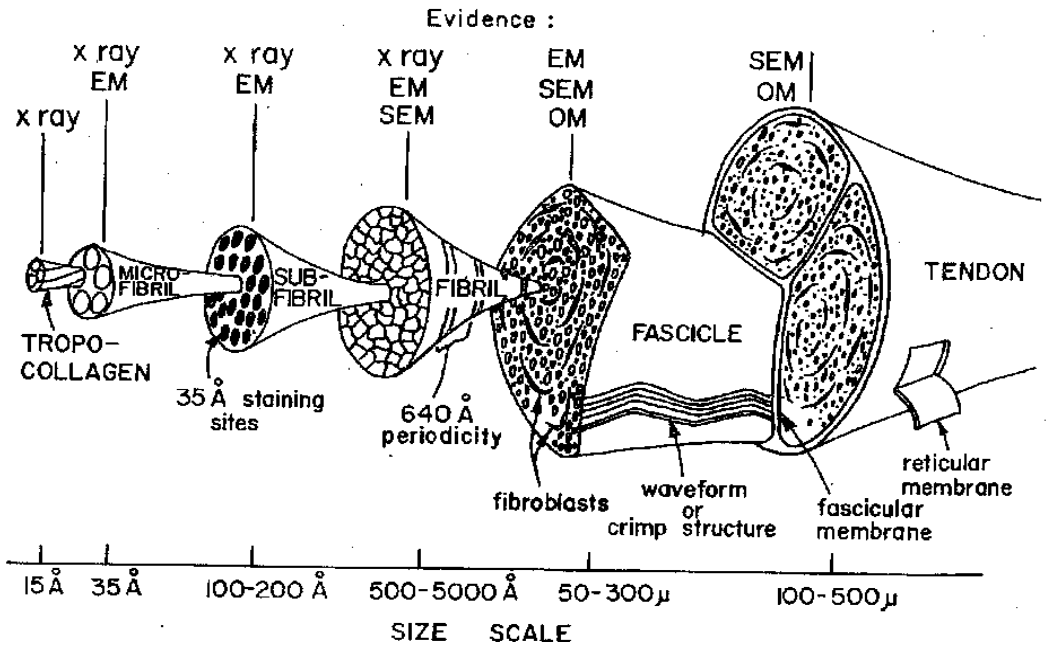

Figure 2.1

Hierarchical structural model of tendon (adapted from Kastelic et al. 1978 with approval)

Methodology

Tissue Retrieval. Four skeletally mature white New Zealand male rabbits were euthanized as part of a separate and unrelated IACUC approved protocol. The rabbits weighed between 3 and 4 kg. Patellar tendons were immediately resected from each animal with a sharp scalpel blade. The desired section was removed from the whole tendon and placed in a fixative solution of ½ strength Karnovsky's (in 0.1M cacodylate buffer pH 7.2) in preparation for TEM. Figure 2.2 shows a schematic of the areas of interest.

Transmission Electron Microscopy. Immediately after the tissue was removed via sharp dissection with a scalpel, it was placed in a fixative solution in

preparation for TEM. Tendons were sectioned in the central center, central proximal, central distal, medial center, and lateral distal sections. Orientation of specimens was maintained by tying a suture to one end. The patellar tendon tissue pieces were fixed in ½ strength Karnovsky's (in 0.1M cacodylate buffer, pH 7.2) for seven days in a 4ºC environment. The tendon specimens were rinsed with a 0.1M sodium cacoldylate buffer (pH 7.2). After rinsing, they were fixed in 1% osmium tetroxide (in 0.1M sodium cacoldylate buffer, pH 7.2) for two hours, and then placed in 1% (aqueous) tannic acid for 1 hour. Thereafter, they were placed in 1% osmium tetra oxide (in 0.1M sodium cacodylate buffer, pH 7.2) for two hours. The tissue underwent two buffer rinses and two water rinses and then was dehydrated in graded ethanol series. The tissue was then infiltrated and embedded in Spur's resin. The sections were cut perpendicular to the longitudinal axis at 75 nm thickness on a Reichert Jung Ultra cut E ultra microtome and viewed on a JOEL JEM 100CXII (JEOL USA, Peabody, MA.) transmission electron microscope at 60 kilovolts. Electron micrographs of 14 equal sized fibril fields within the fascicles of each tendon segment were obtained (20,000 X magnification).

Image Analysis. The fibrils in each image were approximated as being circular in shape. The image areas were 6.4 x 4.3 μ^2 with 242 and 1055 fibrils per image. The digitized TEM images were analyzed using Image J Software (National Institutes of Health, Baltimore, MD). Image J is a public domain

software (inspired by NIH Image) used for image processing and analysis. Image J can display, animate, enhance, analyze and edit images.

Using Image J four images (n=4) were analyzed from the central center portion, three (n=3) from the medial center, two images (n=2) from the central proximal, two images (n=2) from central distal, and two images (n=2) from lateral distal portion. A total of fourteen images were processed, and the fibril number density, area fraction, and diameter distributions were determined from each image. The collagen fibril number density (ND) was calculated using Equation 1; the area fraction of the fibrils was calculated by using Equation 2, and mean fibril diameter was noted as the average size of the fibril diameters within each section. The number density units are fibrils per micrometer squared. The area fraction denotes the percent of fibers within the area of the image analyzed, and the diameter distribution is demonstrated by histograms of frequency versus diameter size (nanometers).

$$NumberDensity(ND) = \frac{TotalFibrilNumber}{Total\,\mathrm{Im}\,ageArea(\mu m^2)} \quad (1)$$

$$AreaFraction(AF) = \frac{TotalFibrilArea(nm^2)}{Total\,\mathrm{Im}\,ageArea(nm^2)} \quad (2)$$

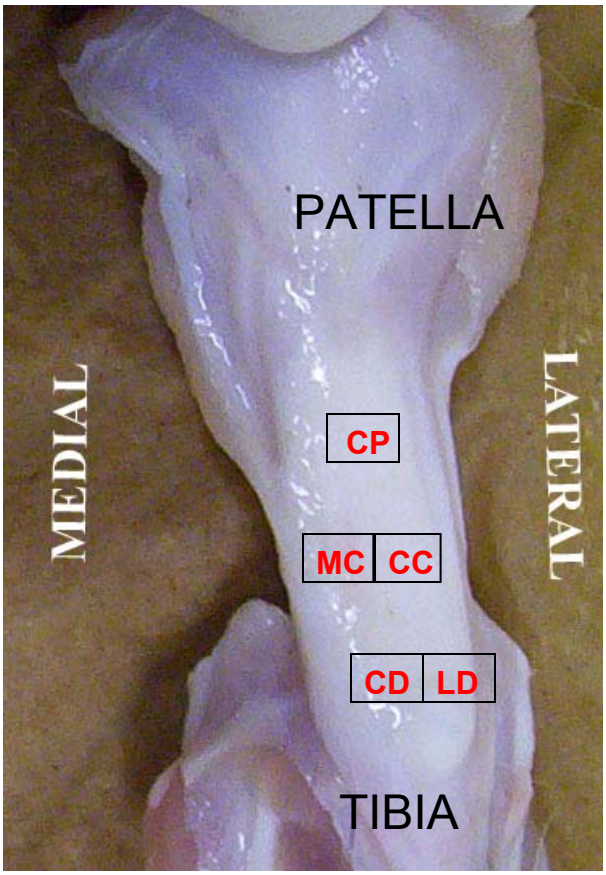

Figure 2.2

Schematic of the areas of interest for microscopy (central center (CC), central proximal (CP), central distal (CD), medial center(MC), and lateral distal (LD))

Statistical Analysis. A univariate (one way between sections) analysis of Variance (ANOVA) method was used to examine the significant microstructural differences based on location. An ANOVA was done to test for differences between areas of interest. For a second statistical analysis, data for areas of interest were pooled in order to compare the proximal, central and distal areas. The population was analyzed with a 95% confidence interval (alpha level set at

0.05), and the Post-Hoc Tukey test was used for quantifying differences between sections.

Results

Figure 2.3 through Figure 2.7 provide representation of the digitized TEM images from each of the processed sections of the tendon. Histograms of fibril frequency versus diameter (nm) were developed for each section of tendon analyzed (Figures 2.8 through 2.13). Table 2.1 lists the fibril number density, area fractions and mean fibril diameter distributions of each examined section. The results show that the central distal section had the smallest fibril number density, the largest fibril diameter and a large area fraction in comparison to the other areas examined. The central center and central proximal sections had fibrils that demonstrated a bimodal distribution. The central distal section had a slight bimodal distribution.

ANOVA was used to test for statistically significant differences based on all locations, showed significant differences between the mean fibril diameters of the central distal section and both the central proximal and lateral distal sections. The mean fibril diameters between the remaining sections were statistically the same.

When the sections were grouped based on their general location (center, proximal, and distal) a significant difference was generated between the center and proximal locations. A weighted histogram of all of the samples was

developed to show the diameter distribution of the compiled sections (Figure 2.13).

The fibril diameter distribution had a range in fibrils sizes from as small as 45 nanometers (central proximal) to fibril sizes greater than 500 nanometers (central center and central distal). Although the fibril diameters are close the results do not show any of the locations to hold exactly the same trend for diameter distribution.

Table 2.1

Mean and standard deviations of number density, area fraction and fibril diameter within the analyzed sections of the tendon.

Tendon Section	Number Density (fibrils/μ^2)	Area Fraction (%)	Mean Fibril Diameter (nm)
Central Center n=4	12 ± 1.6	78 ± 8	257 ± 29
Medial Center n=3	15 ± 3.4	69 ± 5	234 ± 10
Central Proximal n=2	12 ± 0.2	53 ± 5	211 ± 24
Central Distal n=2	10 ± 1.6	69 ± 4	274 ± 24
Lateral Distal n=2	17 ± 7.7	72 ± 9	218.5 ± 20

The following results are characteristic of the samples withdrawn and tested from each section of the tendon. Initially, the processed TEM images are displayed to show the actual fibril arrangement in the specified section, and then the histograms are shown to display the distribution of fibrils within the tissue.

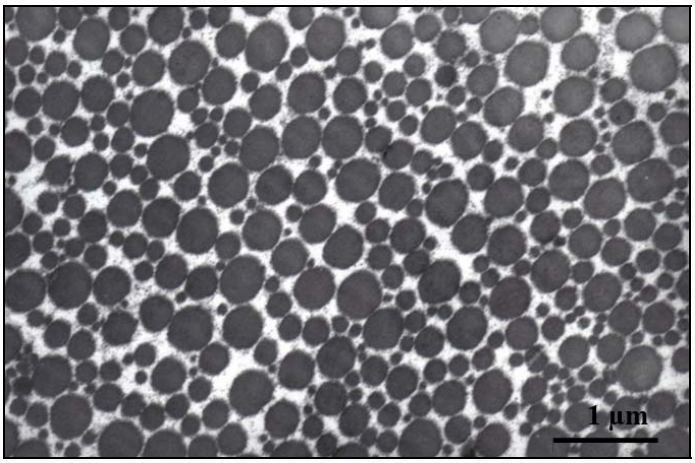

Figure 2.3

Characteristic TEM image of the central center section of the patellar tendon

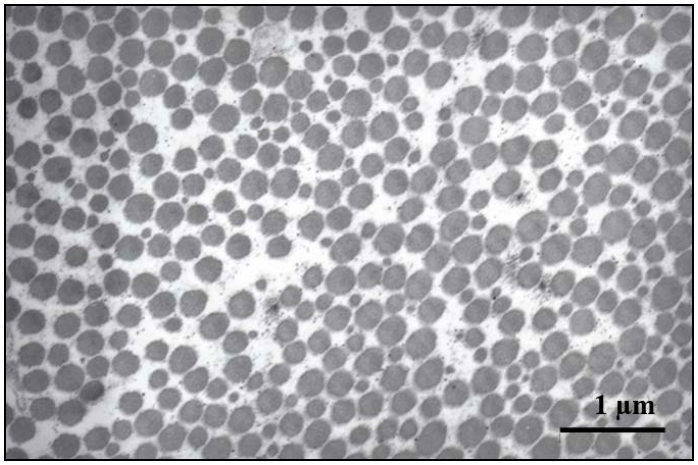

Figure 2.4

Characteristic TEM image of the medial center section of the patellar tendon

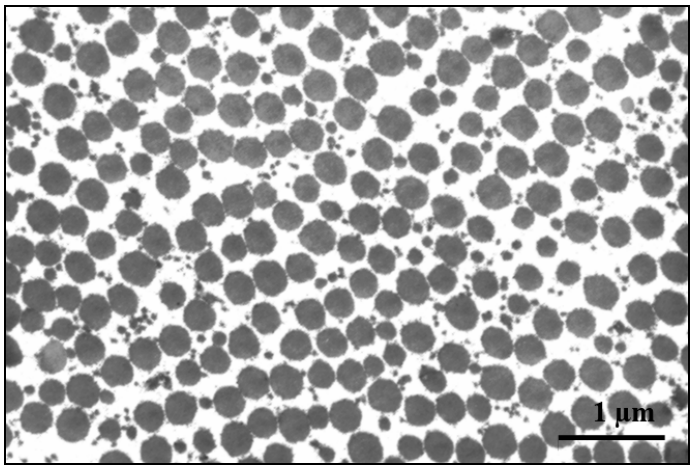

Figure 2.5

Characteristic TEM image of the central proximal section of the patellar tendon

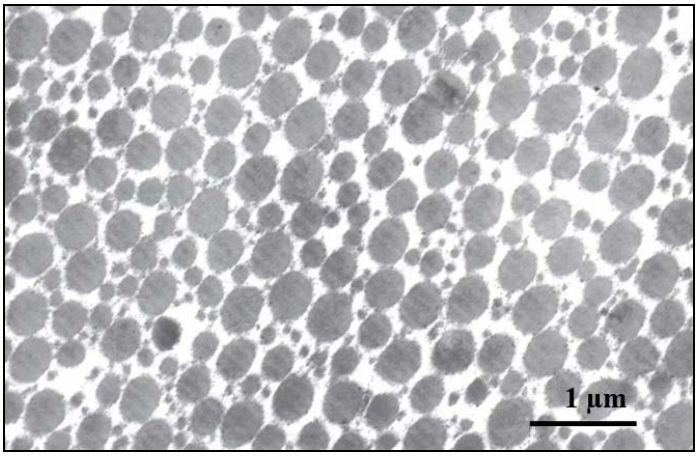

Figure 2.6

Characteristic TEM image of the central distal section of the patellar tendon

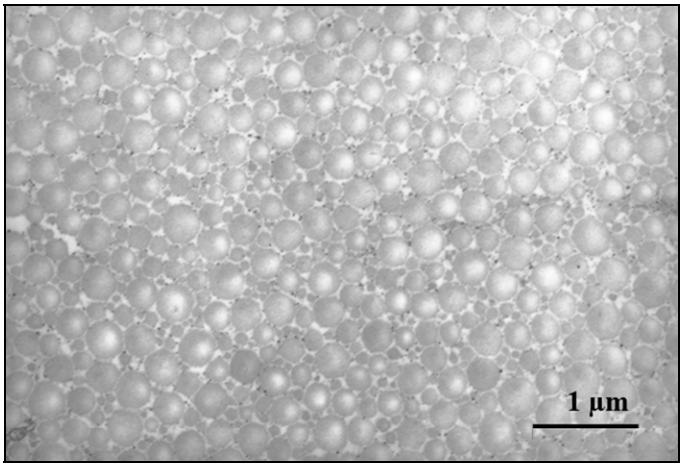

Figure 2.7

Characteristic TEM image of the lateral distal section of the patellar tendon

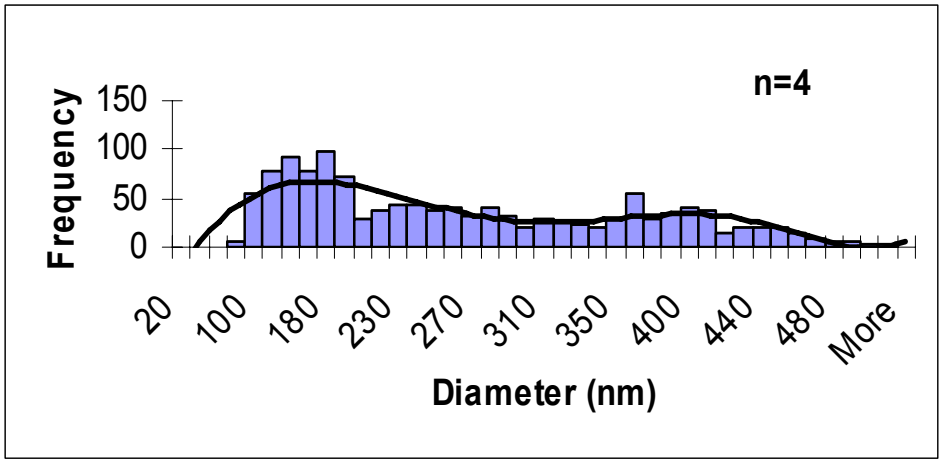

Figure 2.8

Diameter distribution of the central center section of the tendon examined via transmission electron microscopy and analyzed by NIH Scion Digital Image Software

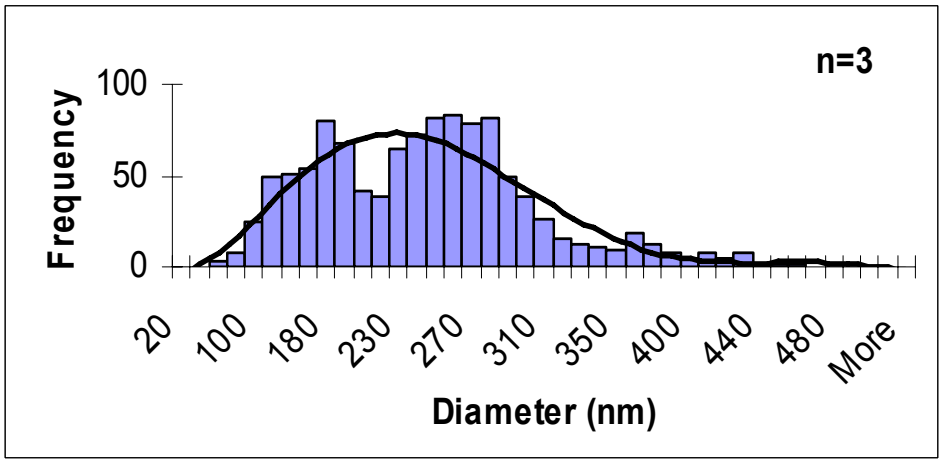

Figure 2.9

Diameter distribution of the medial center section of the tendon examined via transmission electron microscopy and analyzed by NIH Scion Digital Image Software

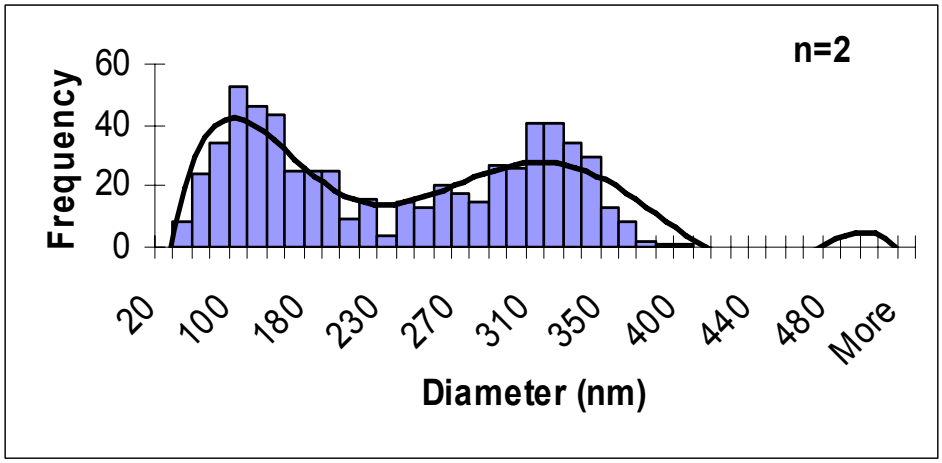

Figure 2.10

Diameter distribution of the central proximal section of the tendon examined via transmission electron microscopy and analyzed by NIH Scion Digital Image Software

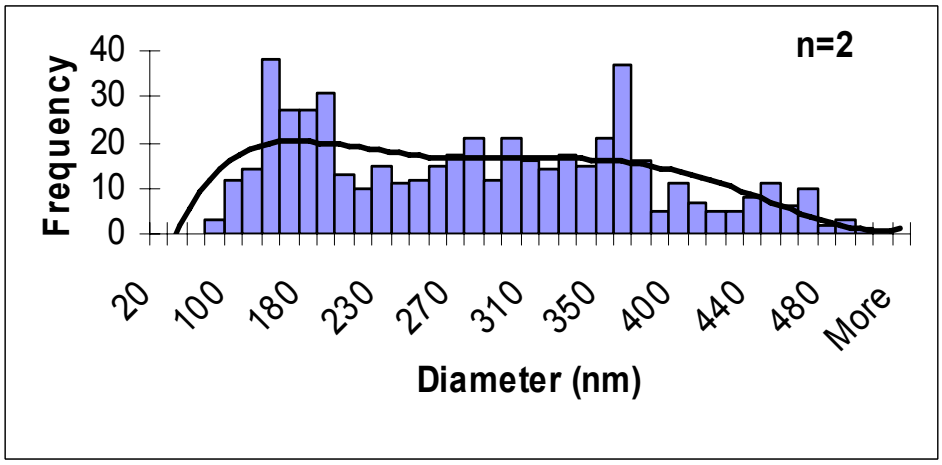

Figure 2.11

Diameter distribution of the central distal section of the tendon examined via transmission electron microscopy and analyzed by NIH Scion Digital Image Software

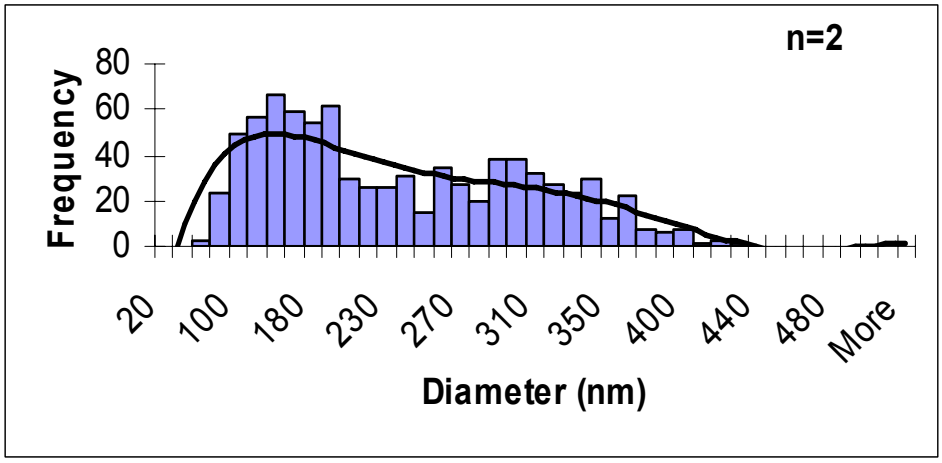

Figure 2.12

Diameter distribution of the lateral distal section of the tendon examined via transmission electron microscopy and analyzed by NIH Scion Digital Image Software

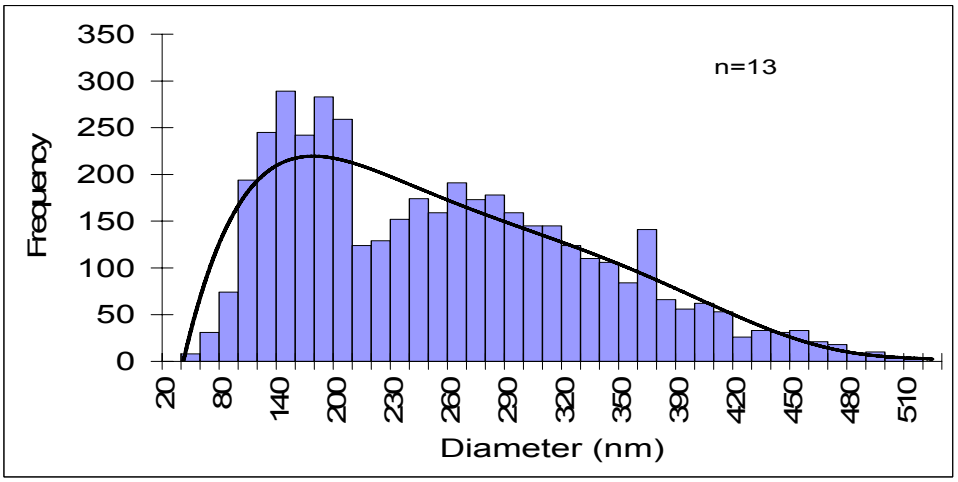

Figure 2.13

Weighted distribution of the sections of the tendon examined via transmission electron microscopy and analyzed by NIH Scion Digital Image Software

Discussion and Conclusion

Conflicting views exist in the characterization and structure-function relationship of collagen fibril diameters in soft tissue. These views cause obscurity in quantification of the mechanical response of the fibrils. For example, Lavagnino et al. (2005) showed that the collagen fibril diameter distribution did not reflect changes in mechanical properties of stress-deprived tendons. However, they did acknowledge that the fibril diameter may contribute to mechanical response to some extent but not by themselves. Frank et al. (1992) showed that ligaments with larger fibrils had a larger failure load, stiffness, stress at failure, and elastic modulus than ligaments with smaller fibers. Derwin's results demonstrated a moderate correlation between the mean fibril diameter and fascicle stiffness (Derwin et al. 1999). Along with the contribution of fibril diameter, Redaelli et al. (2003) showed that proteoglycans play a role in structural-function relationships.

The results of the present study showed that various fibril diameter distributions exist within sections of the tendon. Visual observation of the fibrils in Figure 2.3 through Figure 2.7 shows noticeable differences in fibril size, diameter distribution and area fractions are noticeable. For the central center portion of the tendon, a bimodal distribution for fibril diameter was observed, and it was also apparent that majority of the fibrils were large in diameter. Figure 2.15 is a weighted distribution of all of the sections, and the fibril frequency-fibril diameter relationship is not bimodal, but the cause of this could be a variation in

the number of images analyzed for each section (e.g. n=4 for central center). The weighted histogram shows a larger number of smaller fibrils than that of the larger fibers.

Numerically the central center section of the tendon nearly had the largest mean diameter size out of all sections (just below that of the central distal portion) examined. Along with having one of the largest mean fibril diameters, the central center section had one of the highest area fractions, 78 percent of the section consisted of fibers. Derwin et al. (1999) noted that the area fraction, also referred to as the packing fraction, is directly related to the mechanical output. Parry et al. (1978) stated that the there was a strong correlation between the collagen fibril diameter distribution and the mechanical properties of the tissue. Parry also suggested that a tissue's ability to resist plastic deformation is directly related to the small–diameter fibers and the tissue's ability to withstand high stress levels is related to the percentage of large diameter fibers within the tissue (Parry 1988). Bimodality is indicative of strength within the paralleled fibered soft tissue. This enables the creep inhibition properties of the tissue and the strong tensile properties within the tissue. The central center's large area fraction, large mean fibril diameter and biomodal distribution may be associated with the fact that tendons, most often, fail in their mid-substance rather than at the insertion points. The dense packing of fibrils within the center may serve as a protective mechanism to prevent total tendon failure. Due to the thin nature of the tendon edges, it would likely tear at the edges first and the damage would spread

inward, toward the center. However, when the tear reached the center of the tendon, it provided additional resistance to prevent total breakage.

Collagen fibril area fraction was strongly correlated with failure load, failure stress and modulus in a mouse model (Robinson et al. 2004). Derwin et al. (1999) showed a positive correlation of fibril diameter with load and stiffness. The central center region also had one of the lowest fibril densities or number of fibrils per micrometer squared. Its number density was the same as that of the central proximal portion and slightly greater than that of the central distal portion. Therefore, along the whole central region of the tendon, the number density was consistent. As previously mentioned and as is shown on the TEM images, each of the three segments from the central region of the tendon has bimodality although the central distal portion is only slightly bimodal. Whereas, the other three sections within the tendon did not display bimodality. This could be indicative of the mechanical strength in those areas. The central distal section of the tendon had the greatest mean fibril diameter with a mid range volumetric fraction and one of the lowest number densities. These values were close to that of the central center and may be indicative of the properties along the central section (axial direction). The section with the second highest area fraction was the area closest to the insertion site of the tibia or the lateral distal part of the tendon. The general proximal region within the tendon had the lowest fibril area fractions and mean fibril diameters out of each of the sections. This is likely because only one proximal section was included in this study.

Since this study was a first in examining the microstructure of the rabbit patellar tendon in six specific areas, comparative data was not available for comparison. While Sklenka (2006) did a microscopy study on rabbit patellar tendons and found a statistically significant difference in mean collagen fibril diameter when including location in the analysis, this study did not find a significant difference in mean fibril diameter between all locations. This could possibly be due to the limited number of samples used, which may have contributed to a lower statistical difference. When data were grouped based on the general locations of tendon's center, patellar insertion end, and tibial insertion end (eg. Central Center grouped with Medial Center) an ANOVA showed statistically significant difference between fibril size of the center and proximal sections.

If the data were grouped together in the present study, based on center, patellar insertion (proximal) and tibial insertion (distal), the overall mean fibril diameter of the center portion of the tendon would be the largest, fibrils of the tibial insertion end would be intermediate in size and fibrils of the patellar end would have the smallest mean fibril diameter. Sklenka et al. (2006) included three general locations in their analysis and the authors' primary interest was fibril diameter. Neither number density nor area fraction was measured in Sklenka's study. The central portion of the tendon consistently demonstrated a greater mean fibril diameter, while the patella insertion had fibrils of intermediate

size and the tibial insertion end had the smallest mean fibril diameter (Sklenka et al. 2006).

Overall, this examination showed considerable variation within each section of the tendon. The mechanical properties of tissues are determined by the structural organization of the tissue due to the limited available information of the structure-function relationships of collagen fibrils and the variability within the tendon sections, this study is a first in examining the diversity of tendon structure. The variation is demonstrated by statistically significant differences indicated between three of the five sections (Central Proximal, Central Distal, and Lateral Distal).

Along with considerable variation between sample sections, based on Parry et al. (1978,) Frank et al (1992), and Derwin et al. (1999) studies, we predict that the mechanical properties of the tendon the central center portion's area fraction and diameter distribution may serve as a protective barrier from mid-substance failure. The bimodality within the central section of the tendon confirms its properties. The structure of the central portion of the rabbit patellar tendon includes a high area fraction of fibrils and bimodal distribution of fibril size. This arrangement may provide a protective barrier from mid-substance failure. This study may provide researchers and clinicians with insight into the general distributions of fibrils based on tendon area for developing artificial constructs. Future examinations of each section in the tendon are merited, specifically,

performing mechanical tests at each area of the tendon that was analyzed within this study and verify structure-function relationships.

References

[1] Ateshian, G, Warden, W, Kim, J, Grelsamer, R, and Mow, V (1997) Finite deformation biphasic material properties of bovine articular cartilage from confined compression experiments. Journal of Biomechanics 30:1157-1164

[2] Atkinson, Ts, Ewers, Bj and Haut, Rc (1999) The tensile and stress relaxation responses of human patellar tendon varies with specimen cross-sectional area. Journal of Biomechanics 32:907-914

[3] Derwin, K and Soslowsky, L (1999) A quantitative investigation of structure – function relationships in a tendon fascicle model. Journal of Biomechanics 121:598-604

[4] Frank, C, Mcdonald, D, Bray, D, Bray, R, Rangayyan, R, Chimich, D and N, Shrive (1992) Collagen and fibril diameters in the healing adult rabbit medial collateral ligament. Connective Tissue Research 27:251-263

[5] Kannus, P (2000) Stuctures of the tendon connective tissues. Scandinavian J. Med. Sci. Sports 10:312-320

[6] Kastelic, J, Galeski, A and Baer, E (1978) The Multicomposite Structure of Tendon. Connective Tissue Research 6:11-23

[7] Lavagnino, M, Arnoczky, S, Frank, K and Tian, T (2005) Collagen fibril diameter distribution does not reflect changes in the mechanical properties of in vitro stress-deprived tendons. Journal of Biomechanics 38:69-75

[8] Parry, D, Barnes, G and Craig, A (1978) A comparison of the size distribution of collagen fibrils in connective tissue as a functiion of age and a possible relation between fibril size distribution and mechanical properties. Proceeding of the Royal Society of London B 203:305-321

[9] Parry, Da (1988) The molecular and fibrillar structure of collagen and its relationship to the mechanical properties of connective tissue. Biophysical Chemistry 29:195-209

[10] Redaelli, A, Vesentini, S, Soncini, M, Vena, P, Mantero, S and Montevecchi, F (2003) Possible role of decorin glycosaminoglycans in fibril to fibril force transfer in relative mature tendons – a computational study form molecular to microstructural level. Journal of Biomechanics 36:1555-1569

[11] Robinson, Ps, Lin, Tw, Jawad, Af, Iozzo, Rv and Soslowski, Lj (2004) Investigating tendon fascicle structure-function relationships in a transgenic age mouse model using multiple regression models. Annals of Biomedical Engineering 32:924-931

[12] Sasaki, N and Odajima, S (1996) Elongation of Collagen Fibrils and Force-Strain Relations of Tendons at Each Level of Structural Hierarchy. Journal of Biomechanics:1131-1136

[13] Setton, La and Mow, Vc (1992) A generalized biphasic poroviscoelastic model for articular cartilage: Theory and Experiements. American Society of Mechanical Engineers, Bioengineering Division (Publication) BED 22:589-592

[14] Sklenka, A, Levy, M and Boivin, G (2006) Effect of age on collagen fibril diameter in rabbit patellar tendon repair. Comparative Medicine 56:8-11

[15] Toyhama, H and Yasuda, K (2002) The effect of increased stress on the patellar tendon. Journal of Bone and Joint Surgery (Br) 84:440-446

[16] Yamamoto, E , Hayashi, K, Kuriyama, H, Ohno, K, Yasuda, K and Kaneda, K (1992) Mechanical Properties of the Rabbit Patellar Tendon. Journal of Biomechanical Engineering 114:332-337

[17] Yin, L and Elliott, D (2004) A biphasic and transversely isotropic mechanical model for tendon: Application to mouse tail fascicles in uniaxial tension. Journal of Biomechanics 37:907-916

CHAPTER III

THE ANISOTROPIC COMPRESSIVE MECHANICAL PROPERTIES OF THE RABBIT PATELLAR TENDON

Abstract

Compressive properties of soft tissues are of interest because they are compressed in regions as they wrap around bone. Benjamin et al. (1998) showed the development of fibrocartilaginous matrices in tendons as they wrap around bone. The goal of this study is to contribute insight into the time dependent axial and transverse compressive anisotropic properties of the tendon. Two methods of compression were done in the transverse direction (Methods 1 and 2) and two methods in the longitudinal direction (Methods 3 and 4). Methods 2 and 3 underwent bulk compression and Methods 1 and 4 underwent indentation. The equilibrium modulus obtained for the bulk tests were minimal and therefore this study focused on the equilibrium and instantaneous indentation compressive modulus. The transverse orientations consistently showed an increased modulus with its instantaneous modulus producing the greatest results. Also, a trend analysis shows an exponential increase in modulus based on strain rate.

Introduction

An understanding of multiscale mechanical properties of soft tissue is significance for development of artificial tissue constructs and biologically inspired materials, also known as the science of biomimetics. Specifically, tendon artificial constructs are deemed a necessity due to the fact that approximately 150,000 Americans suffer an injury to their anterior cruciate ligament (ACL) per year (Gentleman et al. 2003). Autografts of the patellar tendon is commonly used as a replacement for the ACL. The ACL replacement results are impaired by limited knee function, and other complications from the autograft. The design of biological tissues is of interest to the engineering community because these tissues "possess structures that span across a full range of length scales in order to react to a variety of environmental stimuli with optimal functionality" (Bruck et al. 2002). Bruck among many others believe that mimicry of the multiscale phenomena between structure and function in soft tissues can contribute to a multitude of technological breakthroughs.

Extensive tensile testing has been performed to understand the mechanical properties of tendon (Woo 1982; Yamamoto et al. 1992; Danto et al. 1993; Johnson et al. 1994; Yamamoto et al. 1998). Mechanical observations have been performed at the macroscale level with much deviation between research groups. Major contributing factors to the large variation in mechanical properties of soft tissues are due to the organization and orientation of collagen fibers as well as the percentages of various constituent materials (Woo, S.L.,

1997). Other experimental variations could be minimized if the experiments are performed in a controlled environment. Therefore, with the long term goal of developing a stress state dependent model (a model that incorporates tension, compression, and simple shear), macroscale testing is important for consistency in data analysis.

As one step toward accomplishing this goal, compression tests were performed to examine the compressive properties of the tendon and compare with tension results and other compression results in the literature. Limited studies are available on the area of indentation and compression testing for examining mechanical properties of the whole tendon and lower length scales of the tissue. In examining literature on compression testing, tests were performed on the supraspinatus tendon due to the need for understanding rotator cuff tears (Lee et al. 2000). Lee determined the compressive stiffness of the bursal and articular sides of the supraspinatus tendon. Indentation testing was conducted on both the bursal and articular sides of the supraspinatus tendon at 0.1mm/s, focusing on the area in which rotator cuff tears often occur. Their results clearly demonstrated material anisotropy in the compressive stiffness as the rotator cuff tendon showed significant differences in stiffness between the bursal and articular sides of the tendon. Zobitz et al. (2001) validated the results of the compressive material properties of the supraspinatus tendon with a finite element model. However, compressive anisotropy was not examined based on fiber orientation.

Compression testing is not commonly applied to tendons, because the tendon primarily functions under tensile axial loading. However, Benjamin et al. (1998) showed the development of fibrocartilaginous matrices in tendons as they wrap around bone and where they attach to bone. In both areas the tendon is under compressive loads. The adaptation process suggests that the cells in tendons are capable of detecting changes in applied mechanical loads and alter the extracellular matrix (ECM) composition accordingly (Benjamin et al. 1998). It is the purpose of this study to illustrate compressive anisotropy and later (in another study) compare the results to tension and shear. The compression testing in this study will serve as model exploration and later assist in the development of a multiscale, multi- stress state continuum model.

Methodology

Eight skeletally mature white New Zealand male rabbits were euthanized as part of a separate and unrelated IACUC approved protocol. Rabbits weighed between 3 and 4 kg. In preparation for the unconfined compression testing, the tendons were thawed and allowed to equilibrate for 30 minutes in 0.9% saline. For one set of tests, eleven replicates of tendons were compressed transverse to the fiber direction. For another set of tests, sixteen replicates were compressed along the fiber direction. Three methods of compression were examined in the longitudinal direction and two methods analyzed in the transverse direction.

Transverse Compression. A small 6 mm indenter was used to test the tendon at various sections (proximal and distal) for Method 1 of transverse

compression. The tendon was positioned so that the indenter directly compressed against the desired region (Figure 3.1). Proximal and distal testing did not occur during the same testing period; each section was tested individually and data collected. For Method 2 of transverse compression, 6 mm diameter circular samples were removed from the proximal and distal ends of the tendon using a dermal punch. The 6 mm pieces were individually compressed with a 20mm diameter platen.

In Method 1, the modulus was not calculated based on Equation 4. The area of the specimens used to calculate the stresses and equilibrium modulus for Method 2 was the same as that of the 6 mm dermal punch (Equation 2). Centerline stress refers to the stress through the tissue area only where indentation occurs. For each method, all specimens were placed in the center of a stainless steel dish filled with saline solution to prevent dehydration. In Method 1, both the proximal and distal sites of the tendon were indented on the tendon. For Methods 2 only one site on the tendon was compressed.

$$A_1 = \Pi * (3mm)^2 \quad (1)$$

$$A_2 = \Pi * (3mm)^2 \quad (2)$$

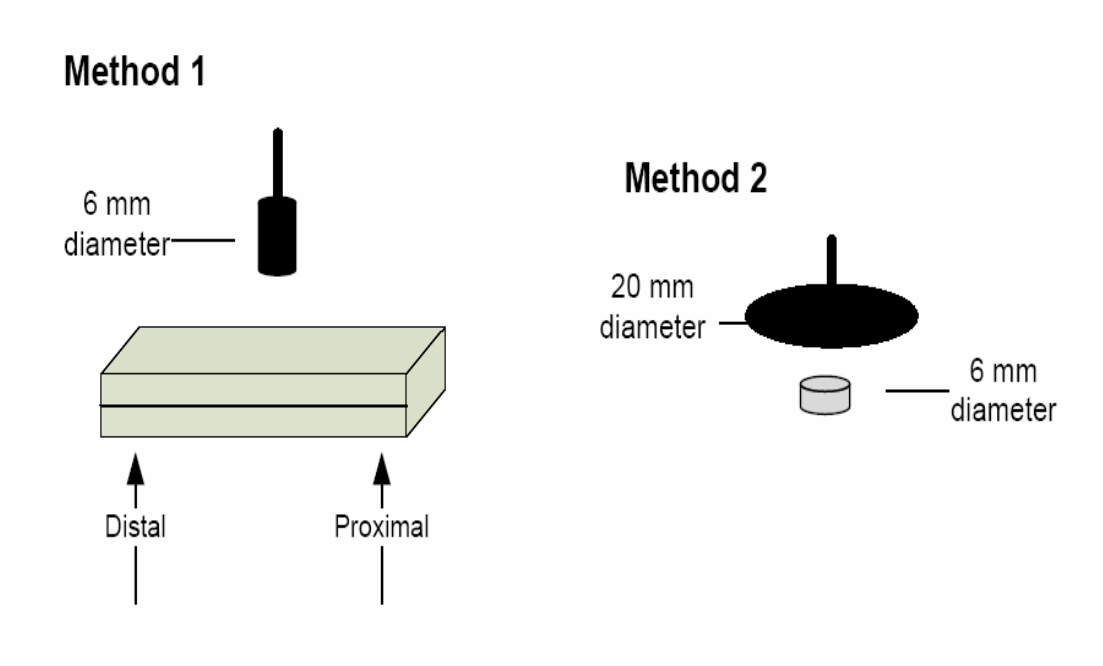

Figure 3.1

Schematic of Methods 1 and 2 compressive testing transverse to the fiber direction

Longitudinal Compression. Portions of the tendon were extracted from the whole tendon using a rectangular steel punch with parallel blades and compressive loads applied with 20 mm diameter platen along the fiber direction. These tests are referenced as Method 3. The tendon sections harvested for longitudinal compression were bonded to a stainless steel cylindrical dish filled with saline solution and compression applied along the fiber direction. For the next set of longitudinal tests (Method 4), rectangular portions were used; however, the specimens were compressed with a 1 mm indenter along the fiber direction. These sections also were bonded to the stainless steel dish for

testing. The cross sectional area of the specimens used in Method 3 was calculated by using NIH image J digital imaging program. A photograph of the image was scanned, the scale was set, and the image was analyzed with the freehand tool. The average area of the specimens used in Method 3 was 37 mm^2. The areas for Method 3 specimens were calculated using Equation 4 to obtain the centerline stress on the tissue.

$$A_5 = \Pi * (0.5mm)^2 \qquad (3)$$

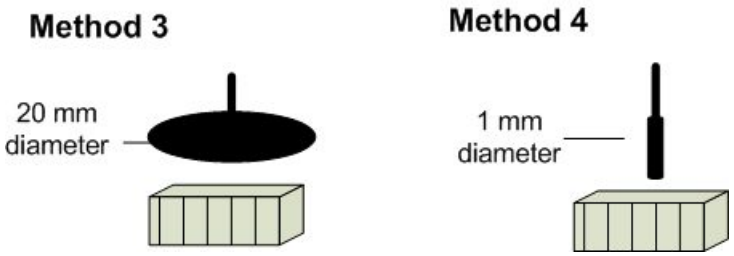

Figure 3.2

Schematic of Method 3 and Method 4 compression testing along the fiber direction

Compression Apparatus. The Mach-1™ (Biosyntech Inc., Canada) micromechanical testing machine was used to apply compression for each method. The experimental setup slightly varied between each method. The primary differences in the setup was the changing of platens and the cyanoacrylate used for longitudinal compression tests. The experimental

environment was in an incubator at 37 ºC, 5% carbon dioxide gas and the protocols were constant for all five methods.

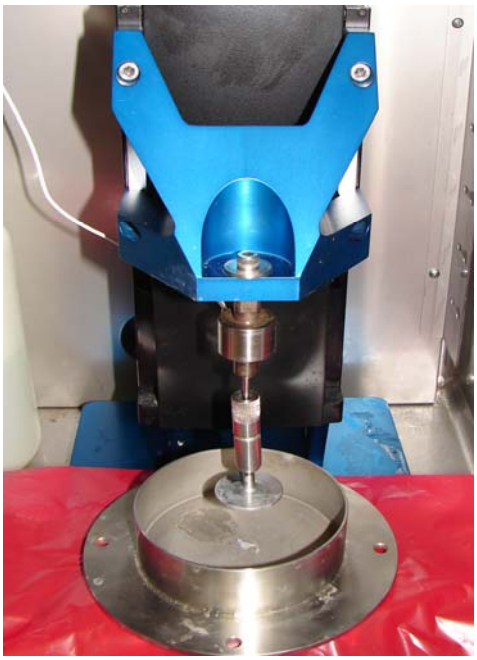

Figure 3.3

Mach I testing devise used for compression testing

*Cross Sectional Area Measurement. T*he area of the specimens used in Method 2 was calculated based on the specimens 6 mm diameter. Images were taken of the specimens used in Method 4 and their areas were calculated using NIH Image J software.

Indentation Equilibrium Compressive Modulus Determination (Methods 1 and 4). Mak et al. (1997) defined the mathematical solution for the indentation modulus of an indenter indenting an elastic half space by using the following equation:

$$E = \frac{P*(1-\nu^2)}{2*A*W} \quad (4)$$

Where P is the load at equilibrium, v is Poisson's ratio of the elastic half-space respectively, A is the radius of the indenter, and W is the depth of penetration of the indenter, which was 1 mm for Methods 1, 3, and 5. Also, Poisson's ratio of the compressed tendon is unknown and therefore two separate values for Poisson's ratio were approximated. Specifically an upper bound limit of 0.5 and a lower bound of 0.1 were used to determine the values which were likely closest to the compressive modulus. Two values of E were obtained and the most reasonable value was chosen. This formulation was used to calculate the modulus for Methods 1, and 4.

Indentation instantaneous compressive modulus determination (Methods 1 and 4). Instantaneous moduli values were determined by using the loads and displacement values at 35% strain. The load value was converted from grams to Newtons and was used as the value for P in Equation 4 and the displacement value was converted from micrometers to meters and used as the value for W in Equation 4. The values were then substituted into equation 4 for modulus determination. The modulus was calculated for a Poisson's ratio of 0.1 and a ratio of 0.5. The instantaneous moduli obtained were then compared to the equilibrium modulus.

Bulk Equilibrium Compressive Modulus Determination (Methods 2 and 3).

To determine the modulus for Methods 2 and 3 the stress relaxation responses were examined from each method and a data point at the equilibrium portion of the curve was captured after every ramp release cycle and plotted. Using Microsoft Excel a linear trend line was fitted to the series of points and the slope of the curve was determined. The slope was noted as the equilibrium compressive modulus of the tissue. Three samples were used in calculating the equilibrium compressive modulus of Method 2 and four samples were used for Method 3. Figure 3.5 is a plot of the equilibrium compressive modulus of one of the specimens within Method 3. The slope (modulus) of the curve is in units of Pascals.

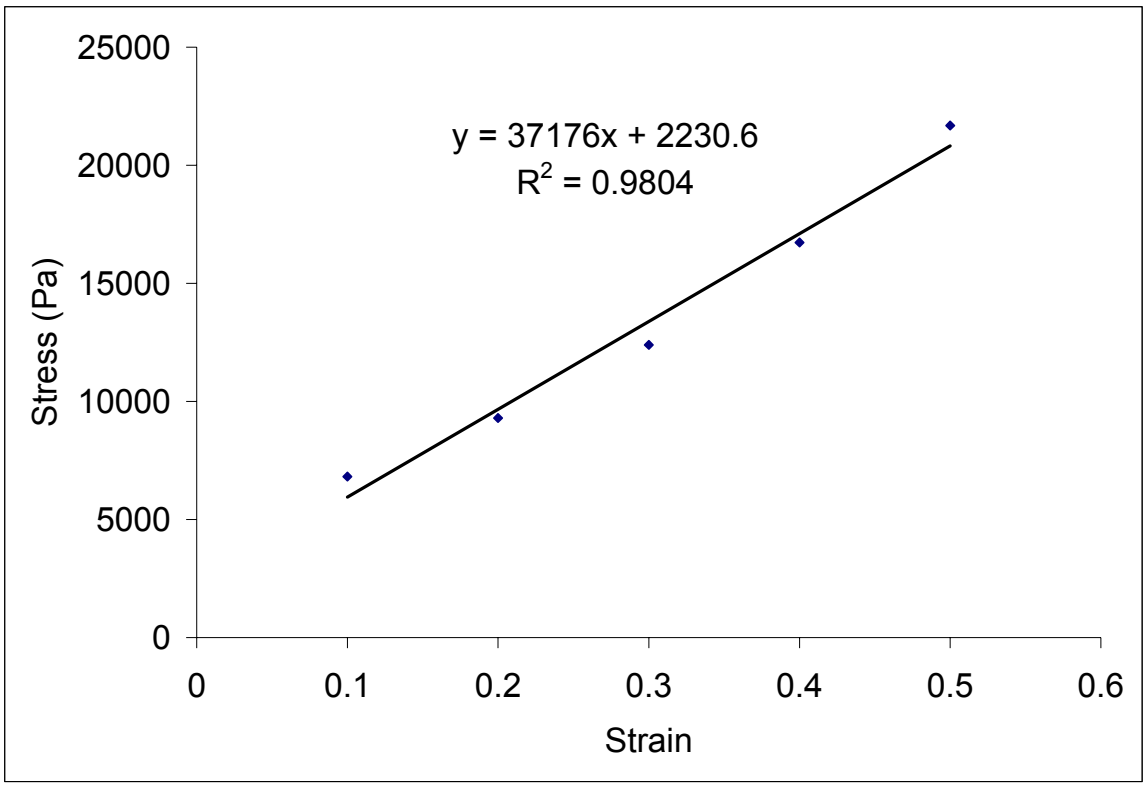

Figure 3.4

Equilibrium modulus determination for Method 2 and Method 4

Tangent modulus versus strain rate (Method 1). Microsoft Excel was used to determine the tangent modulus for the samples used in Method 1. An equation was developed for the curve at 0.1%/s, 1%/s and 10%/s. This was done by fitting the curves with third order polynomial trend lines. The derivatives of the three curves were separately computed and the 35% strain was input into the three derivatives. The values obtained were recorded as the tangent modulus. Figure 3.6 is the graphical representation of the curve fitting for the three strain rates.

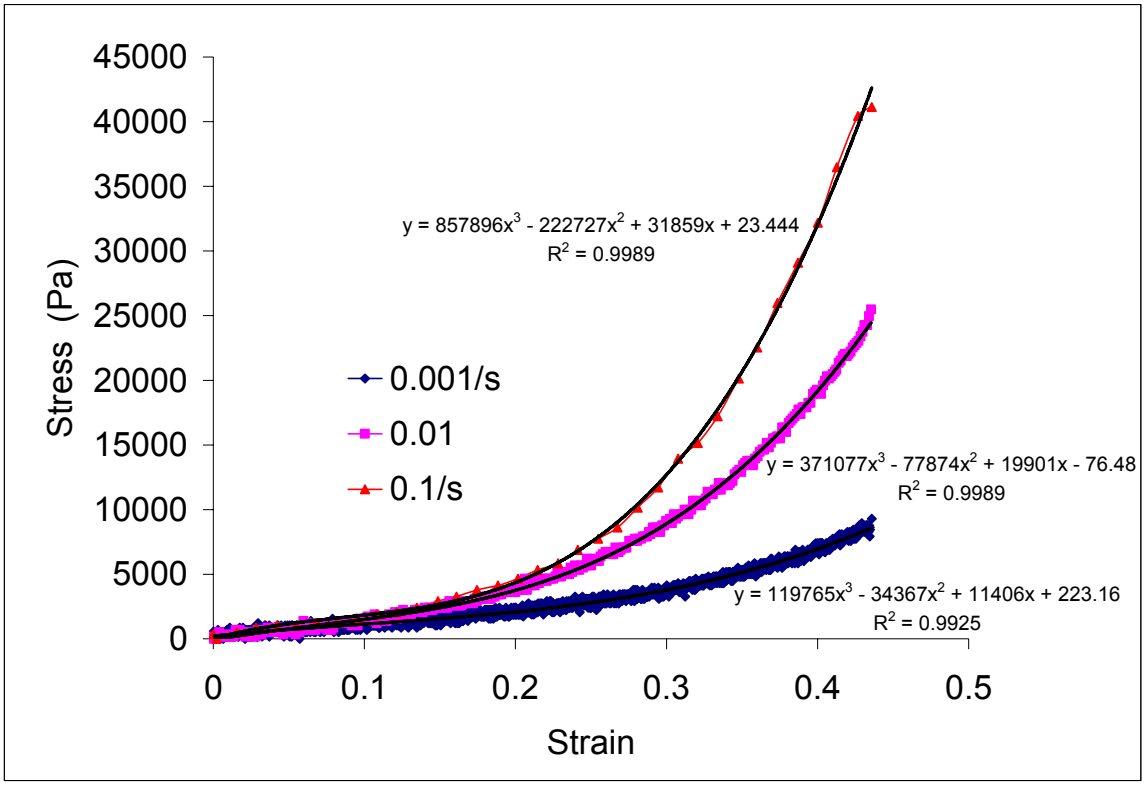

Figure 3.5

Method used to obtain trend of modulus vs. strain rate

Compression Protocol. A program for the Mach I was written that allowed the platen to find contact with the bottom of the dish (flooded with saline) and then find contact with the top of the specimen. The bottom of the dish was recorded as the zero position and the position recorded at specimen contact was the sample thickness. The finding contact step was load controlled and movement was at 10 μm/s, with 100 grams as the stop criterion. The tendon was allowed to equilibrate in saline for 30 minutes before beginning the tests. Stress Relaxation tests began with the ramp amplitude being 10% of the thickness of

the specimen and ramp velocity being approximately 50% of the ramp amplitude with 5 to 7 ramps per specimen. The equilibrium compressive modulus was calculated using the slope of the equilibrium response on the stress relaxation curve (as previously described). The load was removed and the tissue was left to rest and recover for 30 minutes prior to initiating monotonic loading of the specimen. Monotonic loading was applied at 40% thickness at 0.001/s (0.1%/s), 0.01/s (1%/s), and 0.1/s (10%/s) respectively and stress-strain responses were plotted to examine mechanical behavior. Initially the tissue underwent 0.1%/s of strain then 1%/s and finally 10%/s. Thirty minutes of recovery time was allowed between the three different loading rates.

Results

Tables 3.1 and 3.2 list the equilibrium bulk compressive modulus and the equilibrium indentation compressive modulus of Methods 2 and 3 and Methods 1, and 5 respectively. Table 3.3 lists the values of the instantaneous modulus for the indentation tests.

Table 3.1

Equilibrium compressive modulus and standard deviations for the methods subjected to compression in the transverse and longitudinal orientations

Transverse	**Compressive Modulus (kPa)**	**Longitudinal**	**Compressive Modulus (kPa)**
Method 2	9.86 ± 8.58	**Method 4**	1.00 ± 0.84

Table 3.2

Equilibrium compressive modulus for methods subjected to indentation in the transverse and longitudinal orientations

Poisson's ratio= 0.1	**(kPa)**	**Poisson's ratio= 0.5**	**(kPa)**
Transverse--Method 1	16.51 ± 1.50	**Transverse--Method 1**	12.50± 1.13
Longitudinal--Method 4	11.25 ± 3.07	**Longitudinal--Method 4**	8.53 ± 2.32

Table 3.3

Instantaneous Compressive modulus for methods subjected to indentation in the transverse and longitudinal orientations

Method 1		
	Poisson's ratio =0.1	**Poisson's ratio =0.5**
Strain rates 0.001	80.58± 26.69	61.05± 20.22
0.01	237.42± 95.94	179.80± 72.63
0.1	584.62± 509.12	442.90± 385.69
Method 4		
Strain rates	**Poisson's ratio =0.1**	**Poisson's ratio =0.5**
0.001	12.82± 3.70	9.71± 2.80
0.01	21.65± 5.92	16.39± 4.49
0.1	33.11± 17.43	24.99± 13.27

Transverse Compression. Each of the stress relaxation tests in transverse orientation was indicative of the response of viscoelastic tissue. Figures 3.6 through 3.7 are characteristic of the transverse stress-relaxation transverse indentation and bulk compression, respectively. The response of the monotonic loading rates of 0.001/s, 0.01/s and 0.1/s showed the rate

dependency of soft viscoelastic tissues. The rate of 0.001/s had lower stresses for a given strain, with greater stresses at the rate of 0.01/s, and the greatest stresses at a rate of 0.1/s. Figure 3.8 is characteristic of the overall Load displacement response of transverse indentation compression and Figure 3.9 is characteristic of the overall stress-strain response of transverse bulk compression.

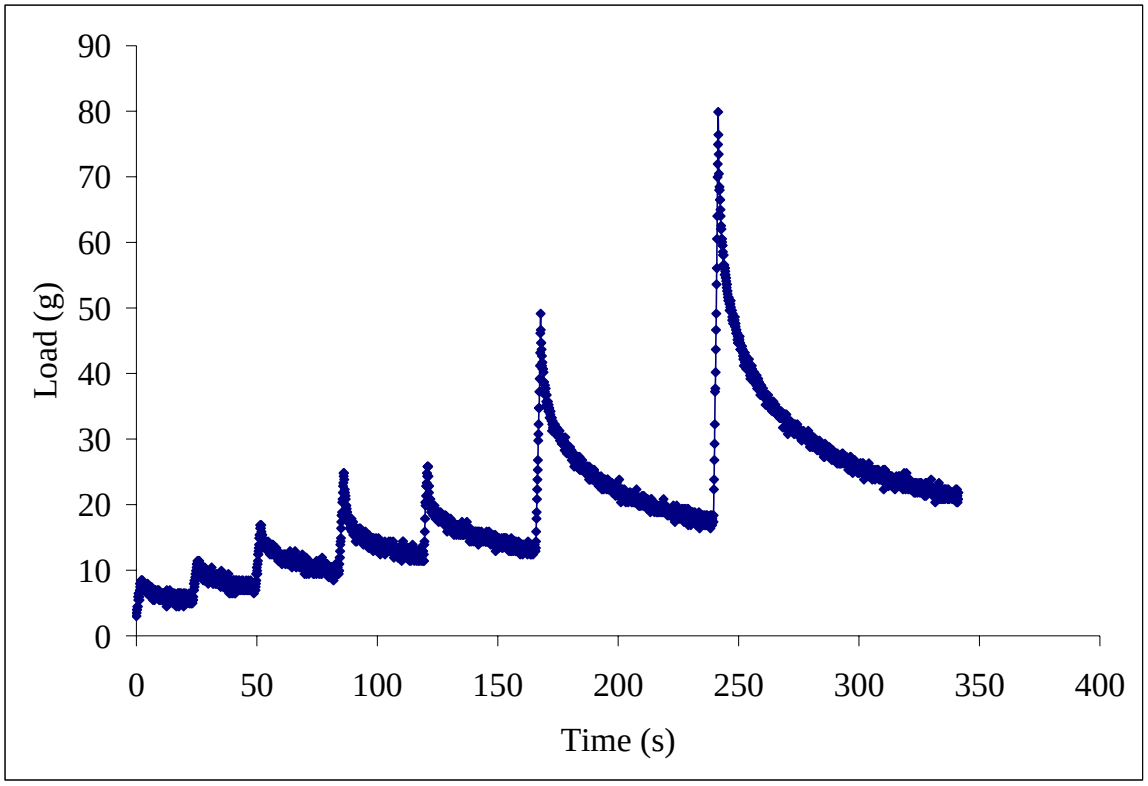

Figure 3.6

Stress relaxation response of tendon undergoing transverse indentation

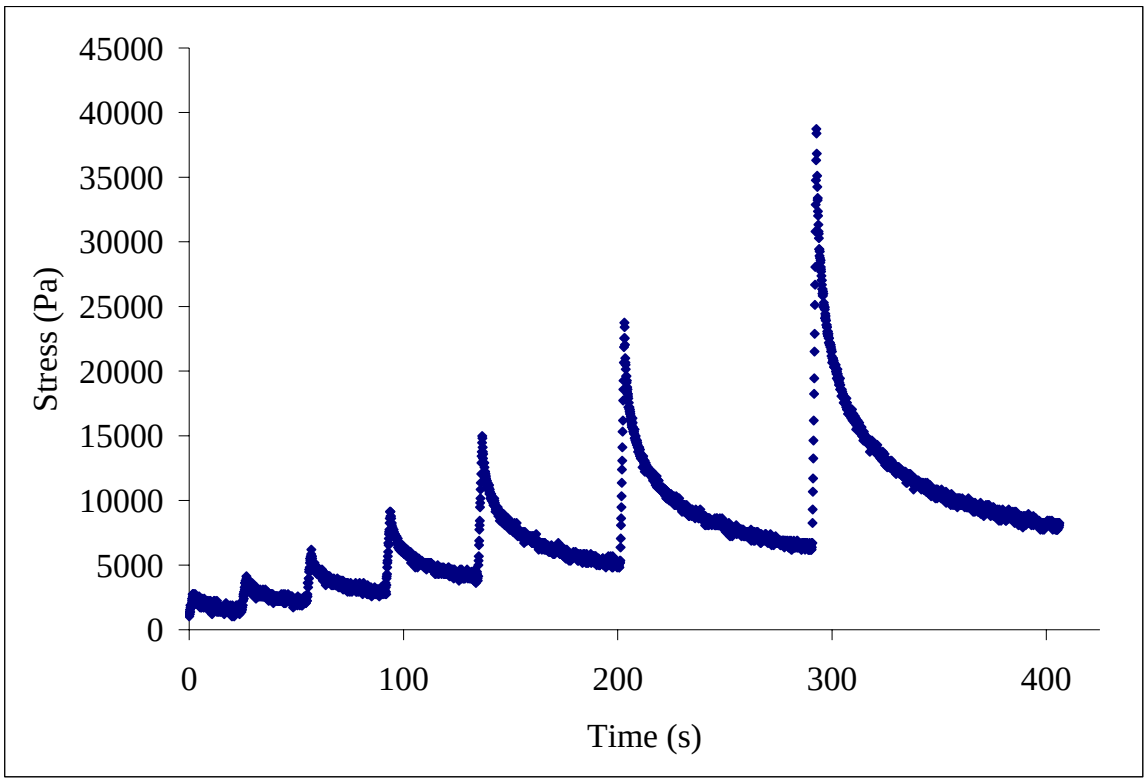

Figure 3.7

Stress relaxation response of tendon undergoing transverse bulk compression

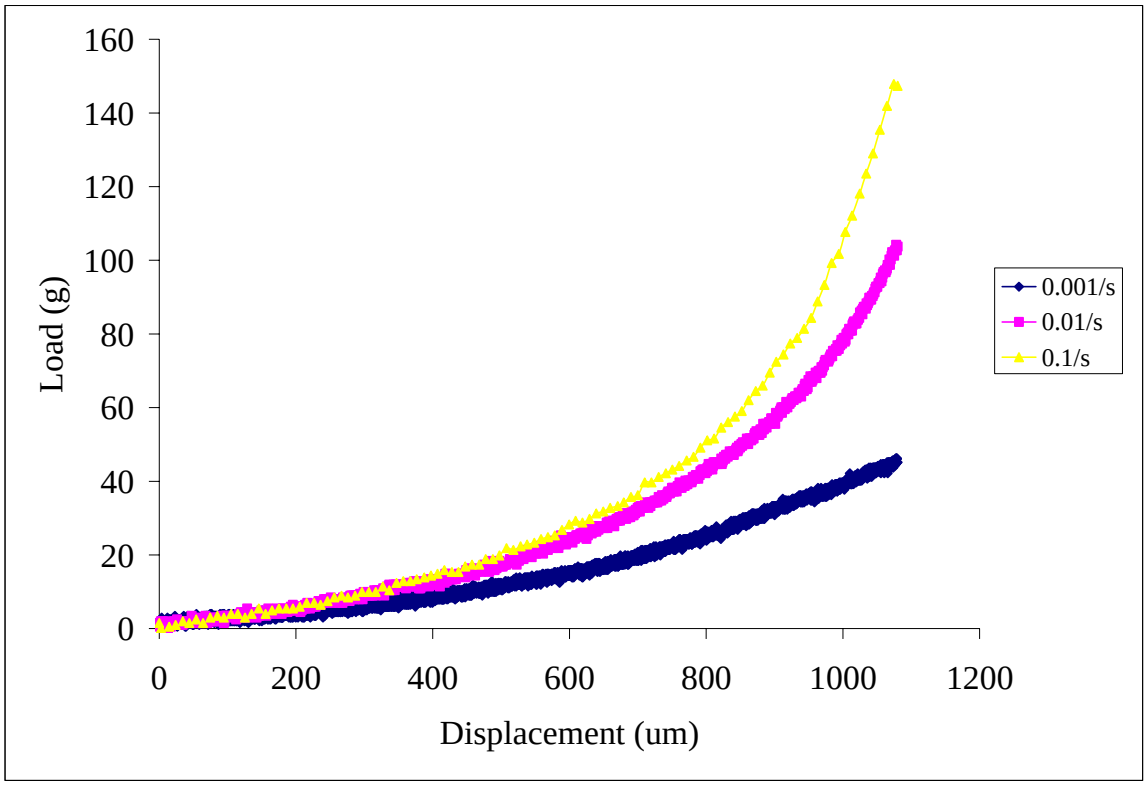

Figure 3.8

Monotonic load-displacement response of rabbit patellar tendon undergoing transverse indentation at three loading rates

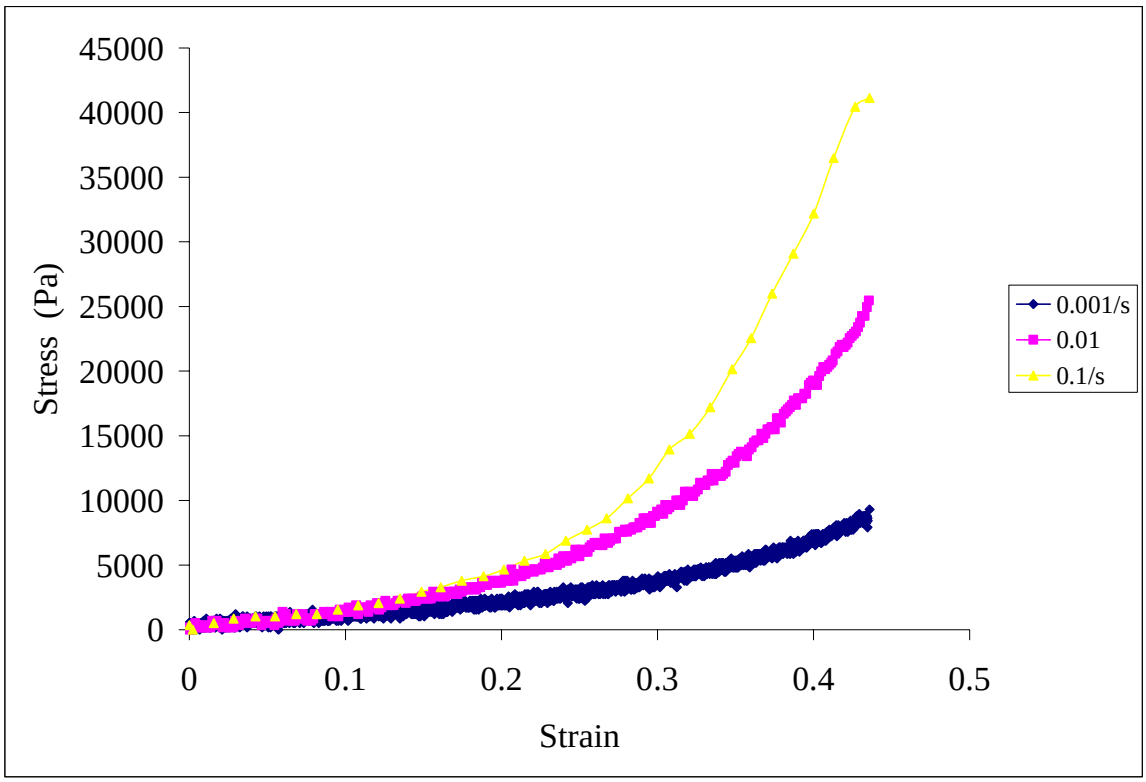

Figure 3.9

Monotonic stress-strain response of rabbit patellar tendon undergoing transverse bulk compression at three loading rates

Longitudinal Compression. Just as with transverse testing, the stress relaxation tests for longitudinal testing were indicative of the response of viscoelastic tissue. Figures 3.10 through 3.11 are characteristic of the stress-relaxation response of each longitudinal study. The responses to the monotonic loading rates of 0.001/s, 0.01/s and 0.1/s showed the rate dependence of the tendon. The loading rate of 0.001/s had lower stresses for a given strain, with intermediate stresses for a given strain at the rate of 0.01/s, and the greatest stresses at the highest loading rate of 0.1/s. Figure 3.12 is characteristic of the overall stress-strain response of longitudinal bulk compression. Figure 3.13 is characteristic of the overall Load displacement response of longitudinal indentation compression

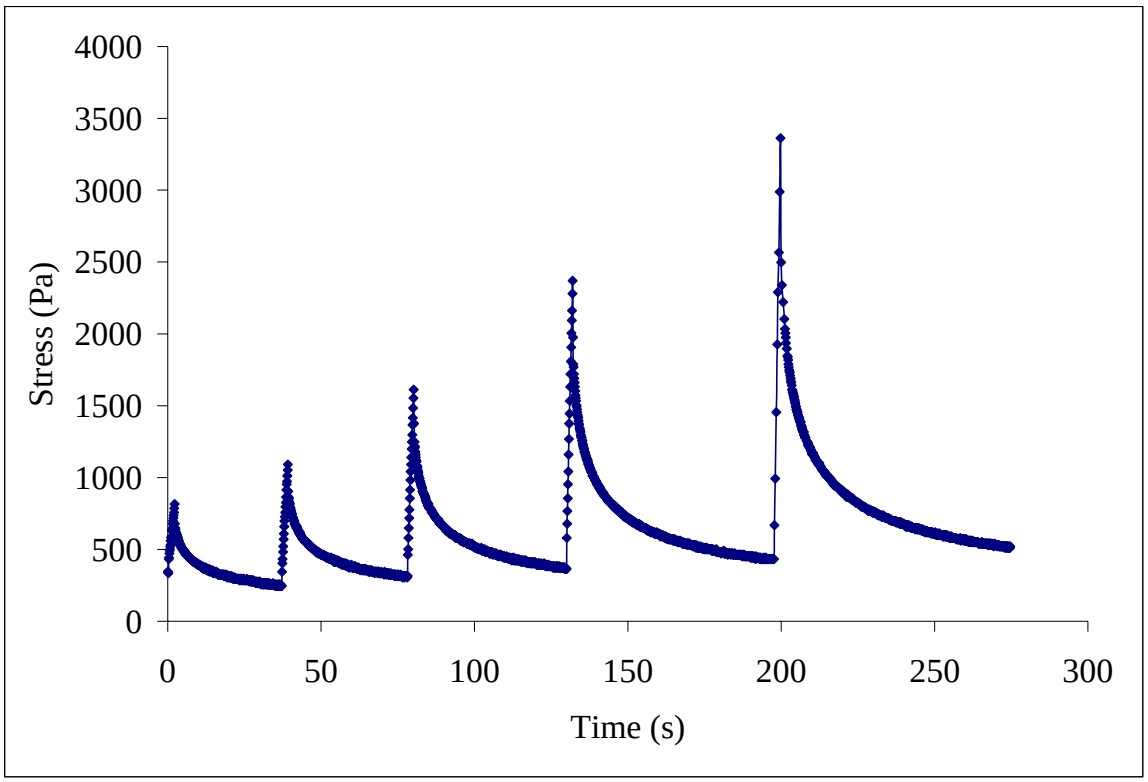

Figure 3.10

Stress relaxation response of tendon undergoing longitudinal bulk compression

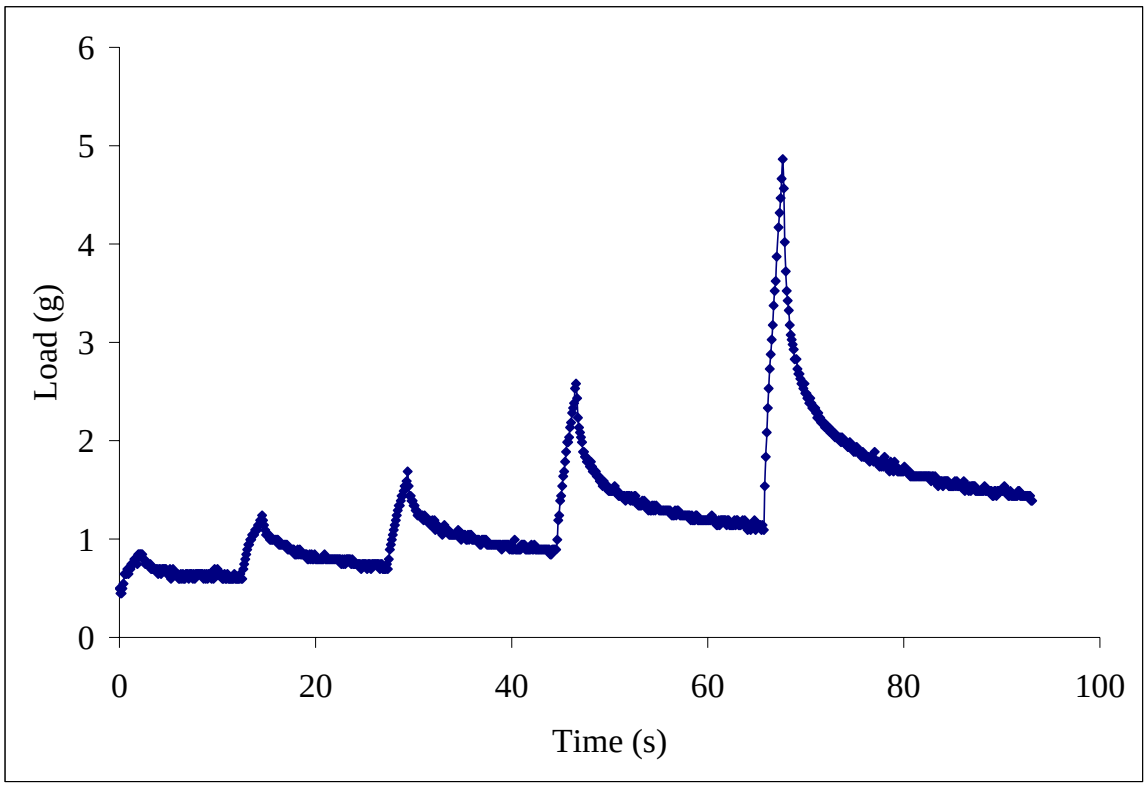

Figure 3.11

Stress relaxation response of tendon undergoing longitudinal indentation

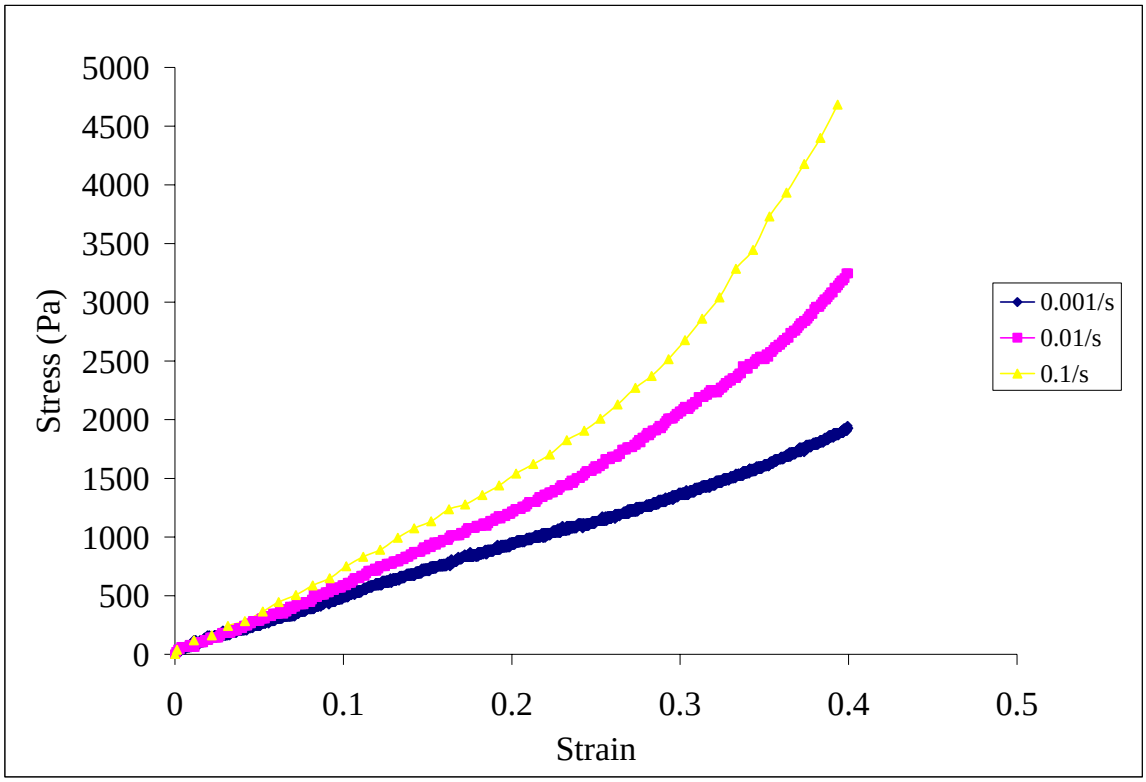

Figure 3.12

Monotonic stress-strain response of rabbit patellar tendon undergoing longitudinal bulk compression at three loading rates

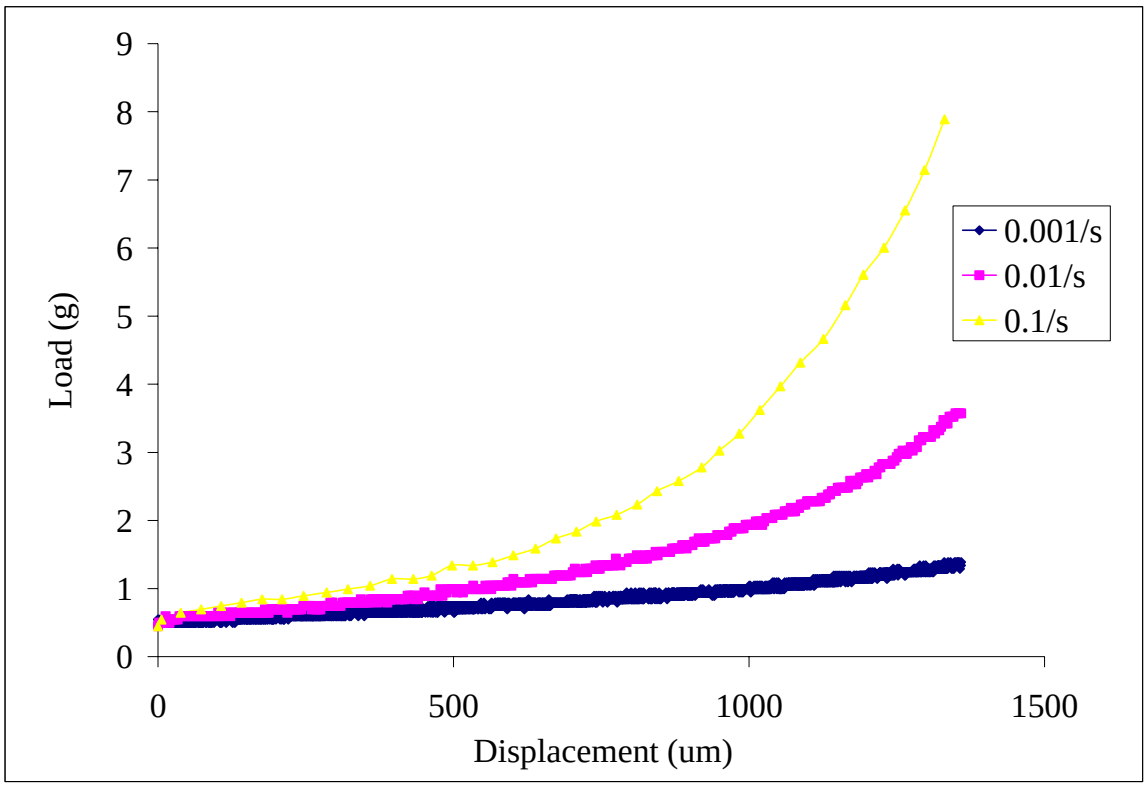

Figure 3.13

Monotonic load-displacement response of rabbit patellar tendon undergoing longitudinal indentation at three loading rates

Transverse vs. Longitudinal Compression. The stress-strain responses of the transverse and longitudinal orientations display the material anisotropy in the tendon (Figures 3.14 -3.15). This confirms the differences in stiffness between the two orientations. The methods chosen for comparison were Methods 3 and Method 5 because similar indentation techniques were performed. The anisotropy is shown at three different strain rates.

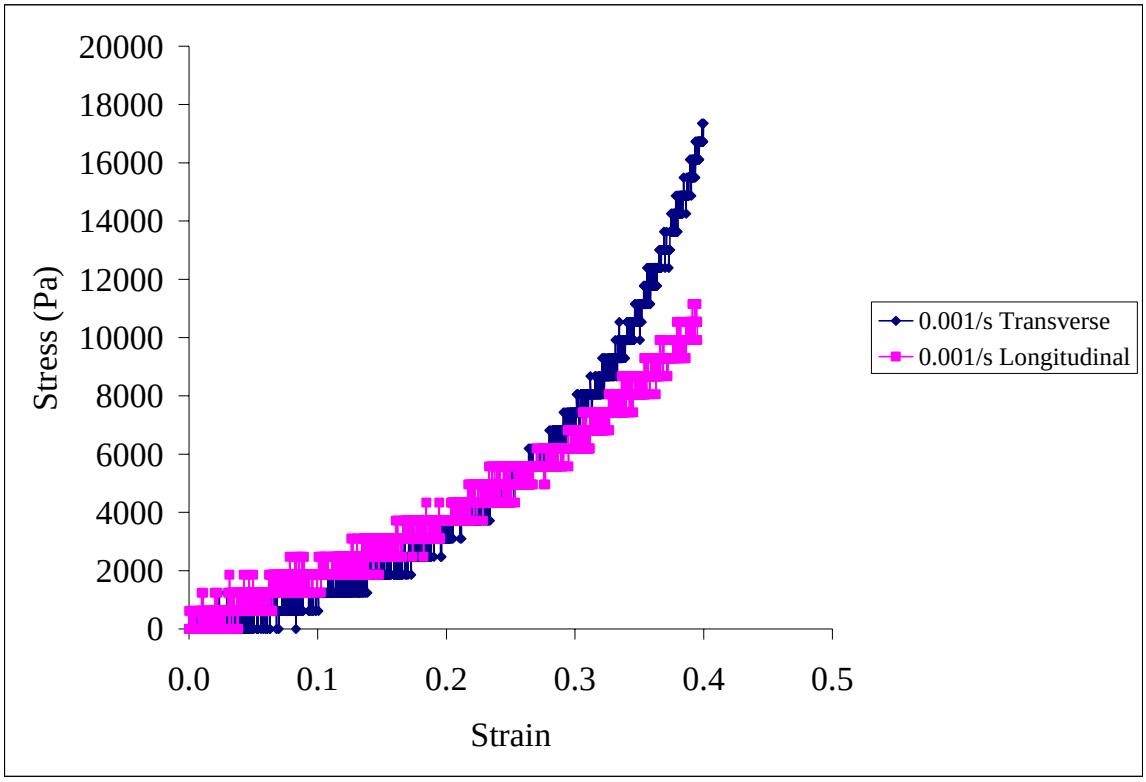

Figure 3.14

A comparison of the stress strain response of the patella tendon of the rabbit during longitudinal and transverse compression at a loading rate of 0.001/s

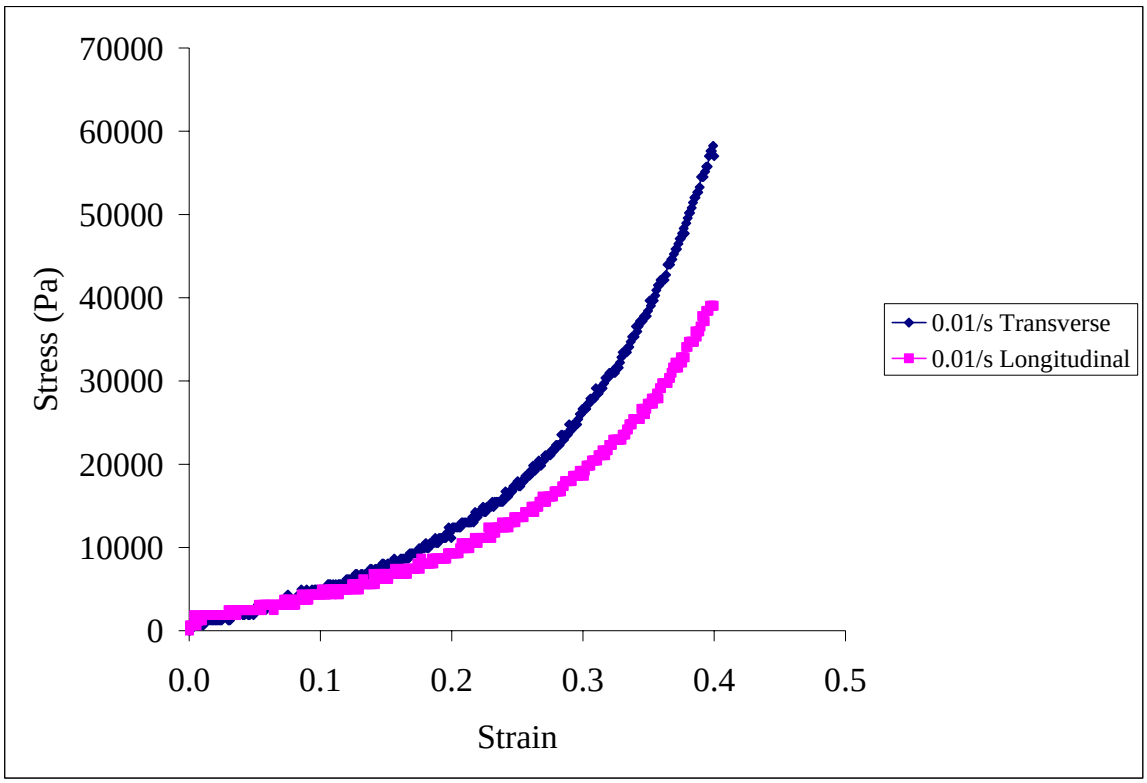

Figure 3.15

A comparison of the stress strain response of the patella tendon of the rabbit during longitudinal and transverse compression at a loading rate of 0.01/s

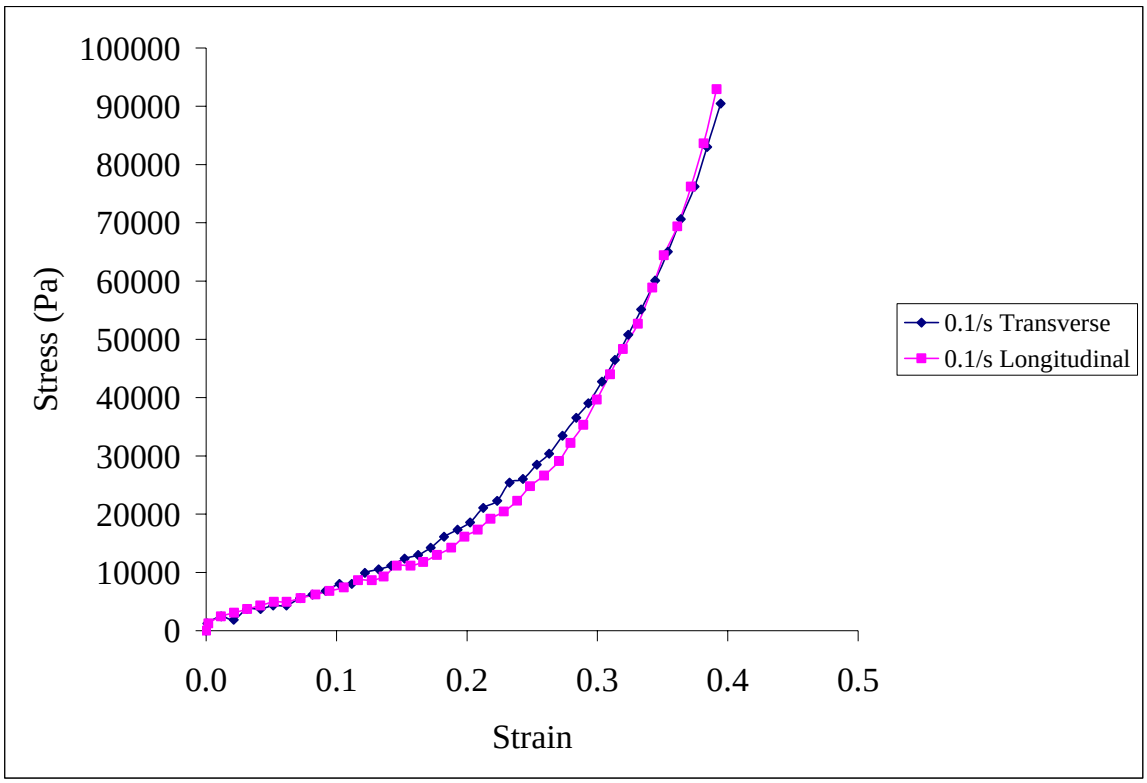

Figure 3.16

A comparison of the stress strain response of the patella tendon of the rabbit during longitudinal and transverse compression at a loading rate of 0.1/s

Tangent Modulus Relationship Based on Strain Rate. Method 1 was used for this analysis because the samples used were whole, intact tendons. In an intact tendon the internal constituents (PGs, GAGs, and proteins) remain in place along with the fluid flow and permit for a near natural environment. Figure 3.17 shows the trend of the tangent modulus. This trend would be the same despite the orientation or strain rate. The response of the tangent modulus vs. strain rate is logarithmic. This response denotes an exponential increase in the tangent

modulus as the strain rate increases. The tangent modulus was obtained at 35% strain from each strain rate.

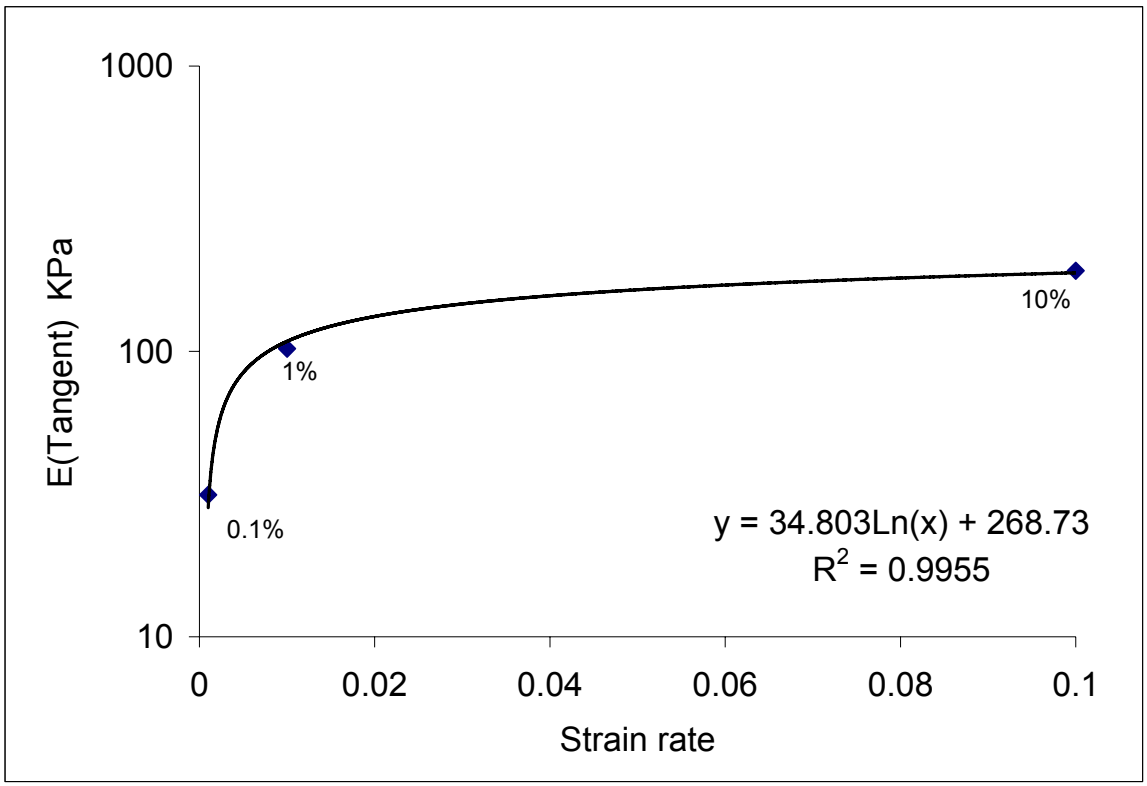

Figure 3.17

Relationship of tangent modulus versus strain rate

Discussion and Conclusion

The compressive stiffness of the supraspinatus tendon was examined by Lee et al. (2000) in order to determine whether regional difference existed in the bursal and articular side of the tendon. There were differences in compressive stiffness between the bursal and articular sides of the tendon. Lee applied compressive stress to the tendon and used an optimization method in Matlab to determine the stiffness of the supraspinatus tendon. Our attempt to determine the stiffnesses in this manner was futile as our optimization procedure did not converge. One specific reason for this problem could be the fact that our input of load and displacement values were much larger than those used in Lee's study and therefore the formulations that Lee et al. developed was not suitable for the rabbit patellar tendon. Lee's study is the primary study in literature on examining the compressive stiffness of tendon and therefore it was important for us to do future studies for the model development.

In the current study, the mechanical response to both transverse and longitudinal bulk compression and indentation is nonlinear. The tendon's high viscoelasticity is denoted by the large relaxation in each strain increment of the stress relaxation responses. Also, the strain rate dependency is evident as monotonic loading at lower strain rates showed considerably less stresses than the stress responses to higher strain rates. Figure 3.17 shows the strain rate dependency on the modulus and the exponential increase in modulus or stiffness as the strain rate increases. The bulk compressive stiffness values are listed in

Table 3.1 and significant variations between the transverse and longitudinal orientations are evident. Most importantly, the values for the bulk modulus directly calculated were low values considering that the compressive modulus for Alginate and Agarose are 5 kPa and 8 kPa respectively (Tew et al. 2005). The actual values of the directly calculated bulk compressive stresses are probably low because of tissue damage due to cutting the tissue into a desired shape. Since the bulk values were extremely minimal, more testing is warranted and the focus of the remainder of the discussion will be towards the properties of the tendons under indentation.

Both the compressive modulus at equilibrium and the compressive modulus based on strain rate (referred to as the instantaneous modulus) were calculated for the indentation methods. The results of the instantaneous modulus were greater than the modulus at equilibrium. Since the modulus and the Poisson ratio of the compressed rabbit patellar tendon are unknown, two Poisson's ratio values were selected to approximate a value that was likely closest to the true compressive modulus. While under compression, visual observation of the tendon showed that a slight bulge exists in the area normal to the applied compression. Although, the magnitude of bulge was not noticeably large, the values of 0.1 and 0.5 were estimated as Poisson's ratio and used to calculate the compressive modulus via indentation. Table 3.2 shows the small variation between the equilibrium modulus for both the longitudinal and transverse orientations. Overall, the equilibrium compressive modulus within the

transverse direction was greater than that of the longitudinal direction. Both orientations have low values at equilibrium. Values of this low magnitude in longitudinal direction could indicate adverse effects on tissue due to processing or the indenter penetrating between fibers and compressing the extracellular matrix.

The results from Table 3.3 show that the instantaneous indentation modulus of the tendons had large variations between orientations. The transverse modulus values were greater than the longitudinal values. As previously mentioned, the equilibrium modulus was low and the instantaneous longitudinal modulus at 0.001/s appeared to approach the equilibrium modulus. However, this was not the case with the transverse modulus. The transverse instantaneous modulus significantly increased from equilibrium. The rate dependency in the modulus is observed in both orientations.

In vivo, tendons primarily are compressed in the transverse direction and they are commonly under tensile stresses in the axial direction. Therefore, this is a probable explanation for the greater compressive stresses and moduli appearing greater in the transverse direction and the larger tensile stresses and tensile moduli along the axial direction. The fact that the transverse samples showed the greatest stiffness may be due to fibrocartilage in tendons as an adaptation to compressive loads. Benjamin provided a detailed explanation of the two major cites on tendon where fibrocartilage is located, mentioned earlier in this manuscript (Benjamin et al. 1998). There are a variety of forms of

fibrocartilage within the tendon; all of these forms have specific characteristics that show a continuous spectrum of tissue between dense fibrous connective tissue and hyaline cartilage. The role of fibrocartilage is to protect the tendon's vasculature. Another cause for the increased values in the transverse direction is the fact that the ECM contains aggrecan which allows tendon to imbibe water when compressed. The imbibing of water may create pseudo-stiffness in the transverse direction.

In their study on the tubelike structure on collagen fibers, Gutsmann et al. (2003) showed that single fibers kink under axial compression. Collagen fibers are more highly crosslinked near the surface and more disordered/soft in the central region, thus kinking occurs. The kinked fibers become straighten when not compressed. This phenonomena may explain the decreased stiffness in the longitudinal direction under both bulk compression and indentation. The fibers may buckle and provide less recruitment under axial compression as opposed to being pulled in axial tension. Also, the breakage of proteoglycans and glycosaminoglycan bonds could destabilize the structure and caused decreased stiffness (Sarkar et al. 1987; Smith et al. 1999).

Along with different orientations, extreme variations in mechanical responses are likely to occur due to the differences in tissue sizes and shapes. Cutting the tissue, as in Methods 2 through 4, may create behavior that does not occur in vivo. For example, fluid flow is a major contributor to tendon viscoelasticity, however, when the tendon is cut the fluid will flow and there will

likely be protein, PGs and GAGs to washout. As a result the mechanical properties of the material would decrease. Bulk compression, along with cutting the tissue may be the cause for a greater decrease in modulus values. For the many reasons aforementioned, the transverse indentation method (Method 1) was chosen to model its response of tangent modulus vs. strain rate. The response of Method 1 indicates that as strain rate increases, the tangent modulus of the tendon increases exponentially. For these same reasons Method 1 will be chosen for implementation into the model. Tew et al (2005) showed the values of alginate and agarose, both of which are near the consistency of gel like substances, as less than 10 kPa. It is known that the tendons overall consistency is much greater than that of a gel like substances. Therefore, it is believed that the values obtained for the longitudinal indentation modulus may have included compression of the gel-like extracellular matrix. Additional indentation testing should be continued in the longitudinal direction with a larger size indenter to prevent direct indenter interaction with the matrix.

This study illustrated the compressive anisotropy of rabbit patellar tendon and is also useful to compare with the tension and shear stress states. Future studies are warranted for examining the transverse compression of the tendon at the proximal and distal ends, where the tissue attached to the bony sections. Also, the stress distribution throughout the tissue is important and therefore finite element methods should be done specifically for indentation testing. Ultimately, the data from Method 1 of this study could be incorporated into a model under

consideration that the trend from both transverse and longitudinal testing showed clear evidence of the viscoelastic properties of soft tissue and the modulus was in reasonable range.

References

[1] Benjamin M and Ralphs J (1998) Fibrocartilage in tendons and ligaments--an adaptation to compressive load. Journal of Anatomy 193:481-494

[2] Bruck H, Evans J and Peterson M (2002) The role of mechanics in biological and biologically inspired materials. Experimental Mechanics 42:361-371

[3] Danto M and Woo S (1993) The mechanical properties of skeletally mature rabbit anterior cruciate ligament and patellar tendon over a range of strain rates. Journal of Orthopedic Research 11:58-67

[4] Gentleman E, Lay A, Dickerson D, Nauman E, Livesay G and Dee K (2003) Mechanical Characterization of Collagen Fibers and Scaffolds. Biomaterials 24:3805-3813

[5] Gutsmann T , Fanter G , Venturoni M, Ekani-Nkodo A , Thompson J , Kindt J, Morse D , Fygenson D. K and Hansma P (2003) Evidence that collagen fibrils in tendons are inhomogeneously structured in a tubelike manner. Biophysical Journal 84:2593-2598

[6] Johnson G, Tramaglini D, Levine R, Ohno K, Choi N and Woo S (1994) Tensile and viscoelastic properties of human patellar tendon. Journal of Orthopedic Research 12:796-803

[7] Lee S, Nakajima T, Luo P, Zobitz M, Chang Y and An K (2000) The bursal and articular sides of the supraspinatus tendon have difference compressive stiffnesses. Clinical Biomechanics 15:241-247

[8] Mak A, Lai W and Mow V (1987) Biphasic indentation of articular cartilage-I. Theoretical analysis. Journal Biomechanics 20:703-714

[9] Sarkar S, Hiyama C, Niu C, Young P, Gerig J and Torchia D (1987) Molecular dynamics of collagen side chains in hard and soft tissues. A multinuclear magnetic resonance study. Biochemistry 26:6793-6800

[10] Smith B, Schaffer T, Viani M, Thompson J, Frederick N, Kindt J, Belcher A, Stucky G, Morse D and Hansma P (1999) Molecular mechanistic origin of the toughness of natural adhesives, fibres and composites. Nature 399:761-763

[11] Tew G, Sanabria-DeLong N, Agrawal S and Bhatia S (2005) New properties from PLA–PEO–PLA hydrogels. Soft Matter 1:253-258

[12] Vlassak J and Nix W (1993) Indentation modulus of elastically anisotropic half spaces. Phiolosophical Magazine A 67:1045-1056

[13] Woo SL (1982) Mechanical properties of tendons and ligaments. Biorheology 19:385-396

[14] Yamamoto E , Hayashi K, Kuriyama H, Ohno K, Yasuda K and Kaneda K (1992) Mechanical properties of the rabbit patellar tendon. Journal of Biomechanical Engineering 114:332-337

[15] Yamamoto N and Hayashi K (1998) Mechanical properties of rabbit patellar tendon at high strain rate. Bio-Medical Materials and Engineering 8:83-90

[16] Zobitz M, Luo Z and An K (2001) Determination of the compressive materials properties of the supraspinatus tendon. Journal of Biomechanical Engineering 123:47-51

CHAPTER IV

A PRELIMINARY EXAMINATION OF STRUCTURAL CHANGES OF THE TENDON PULLED IN TENSION

Abstract

In vivo, generated mechanical forces influence and modify the basic structure of biological tissues. This change in structure could be affected by various sources of internal forces, many of which have yet to be determined. The primary purpose of this study was to subject rabbit patellar tendon to various levels of strain,3 %, 4% and 6%, and quantify the microstructural changes within the rabbit patellar tendon through transmission electron microscopy. The data will be used to validate a multiscale microstructural model. Each of the treatments in this study demonstrated a unimodal diameter distribution and similar quantitative results were observed in this study for the three pulled tendon specimens. Large area fractions and mean fibril diameters were quantified for the pulled specimens. The tendon pulled at 6% showed higher loads and evidence of collagen fibril failure. The variation in the mechanical response of each tendon is a result of the underlying mechanisms of the tendon. Further examinations into this testing are required for definitive results.

Introduction

The tendon, a complexly designed biological structure, is viscoelastic in nature and displays nonlinear, anisotropic and inhomogeneous characteristics (Butler et al. 2000). The basic unit of the tendon is collagen and, within the collagenous matrix, there are many cells and macromolecules that assist with development of the tendon into a complete structure. The intermolecular cross-linking and chemical structure of collagen, its interaction with the ground substance within the tendon, and the hydrophilic attributes of the macromolecules and collagen fibers are all contributors to the mechanical characteristics of the tendon (Woo et al. 1997). Viidik (1980) stated that collagen's main physiological functions within the tissues of the body are to (1) function primarily in a protective and stabilizing manner and (2) serve as an important link between components of the locomotive system. Therefore, the cross linking of each collagen fiber and fiber bundle within the tendon confers upon it high tensile strength and flexibility. This enables the tendon to perform its function of allowing joint movement.

Structure-function relationships of tendons and other biological materials have become increasingly important due to the need for the development and manufacturing of functionally engineered constructs required for tissue repair or replacement. The tendon's highly complex organization has made it difficult to correlate the relationship of structure with function. The material properties are important in predicting the mechanical response of a tissue subjected to various

loading histories (An 2005). Elliot (1965) analyzed the macro structure-property of the tendon and its function as it related to its attachment to muscle and its enabling of joint movement; however, this work is not informative on internal microstructure and functional properties. In Kastelic's examination of the tendon, the hierarchical structure was observed through material analysis with scanning electron microscopy (SEM) (Kastelic et al. 1978). This study was one of the first to show the tendon's structural hierarchy along with cross sectional details. Many studies were conducted as a result of this detailed information on the tendon.

Parry (1988) studied on the molecular and fibrillar structure of collagen and its relationship to the mechanical properties of connective tissue, and provided in-depth information on the role of the collagen fibril in the tendon and its importance to the function of the tendon. Derwin studied the structure-function relationships in a tendon model and showed the positive correlation between fibril diameter and stiffness (Derwin et al. 1999). In Robinson's study on structure-function relationships, it was indicated that fibril area fraction was a significant predictor of failure load, failure stress, and modulus (Robinson et al. 2004). Under varying percentages of strain, the tendon experiences internal stresses on its fibers. In 1931, Nauck was the first to report visible changes within the tendon while subjected to tensile loading (Elliott 1965). This difference was noted along the longitudinal fiber direction. The group showed that the waviness disappeared when tension was applied. In 1958,

Rigby et al. showed, using in rat tail tendons, that this waviness became straight before a strain level of 3% was reached (Rigby et al. 1958). These outcomes show the importance of microstructural properties; therefore, when evaluating at lower scales, one must bridge the length scales to account for total deformation or structural change. Evaluation at lower structural scales may provide future insight into macroscopic damage and failure mechanisms. Additional work is warranted to assist in the contribution to and the understanding of the property relationships.

The literature has shown that the stress in the tendon, when pulled in tension, behaves differently than when subjected to compressive loads. While under tensile strain, the histological findings of Tohyama et al. (2002) showed that a moderate stress enhancement caused a slight delay of the infiltration of extrinsic cells from surrounding tissues into the tendon. Overall, their study showed that doubling the physiological stress resulted in deterioration in the tensile strength and disorganization of the collagen bundles. The reasons for this behavior could be (1) the exudation of fluids (Hannafin et al. 1994) and (2) the morphological change of the tendon cells (elongation) when the tendon is subjected to tensile strain, which plays a significant role in the mechanical signal transduction pathway (Arnoczky et al., 2002). Hannafin et al. (1994) showed that more water was extruded from the tendon during the time when load was applied compared to the amount of water imbibed when load was relaxed. Therefore, if recovery time is not long enough the result is a net decrease of tissue water over

time. The creep in the tendon results in an increase in fibril packing and may cause a decrease in the unbound water space and limit the total water content of the tendon (Hannafin et al. 1994). This phenomena leads to decrease in viscoelasticity and ultimately repetitive loading induced failures. Both, the exudation of fluids and the morphological change of the tendon cells (cell elongation) may contribute to the tendon having a fiber aligned Poisson's ratio value greater than 0.5, which indicates a volume loss from the tissue. In an evaluation of Poisson's ratio of the tendon, Lynch et al. (2002) showed the fiber aligned Poisson's ratio in the longitudinal direction to be approximately 3, which was much larger than in the transverse direction (less than 1).

From the mechanical aspect, Yamamoto reported that the rabbit patellar tendon failed at approximately 6 % strain (Yamamoto et al. 1992). In their examination of the bovine Achilles tendon, Sasaki et al. (1996) showed that the tendon failed at 6 % strain. Therefore, It is the goal of this study to contribute to further understanding of the structure function relationship of the tendon by subjecting it to tensile loading under both subfailure (3 % and 4 % strains) and failure conditions (6 % strain) and capturing its variation in structural properties using transmission electron microscopy (TEM).

Methodology

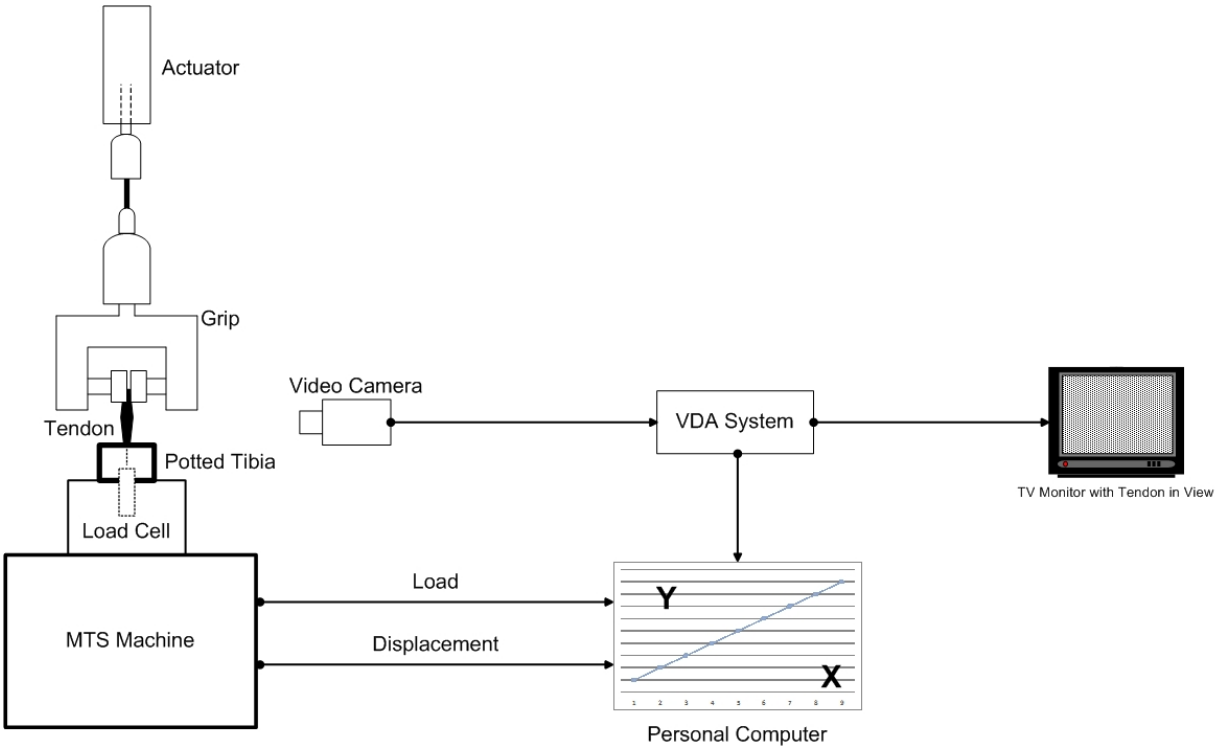

Figure 4.1

Schematic of setup for tension testing

Tissue Retrieval. Eight skeletally mature white New Zealand male rabbits were euthanized as part of a separate and unrelated IACUC approved protocol. Rabbits weighed between 3 and 4 kg. The patella-tendon-tibia complex was removed from the rabbit following euthanasia. The complexes were mounted on the MTS and subjected to load. Each patella-tendon-tibia complex underwent mechanical testing and was immediately resected with a sharp scalpel blade. Following testing, the central center section of the tendon was removed from the

whole tendon and placed in a fixative solution of ½ strength Karnovsky's (in 0.1M cacodylate buffer, pH 7.2) in preparation for TEM.

Mechanical Testing. The patellar-tendon-tibia complexes were thawed and set up to undergo tension testing on an MTS 858 (MTS, Eden Prairie, MN) mechanical testing machine. In preparation for mechanical testing, both the muscle and fat tissue were removed completely from the tibia and the fat tissue removed from the tendon. Prior to potting the tibia in an acrylic resin (Jorgensen Laboratories, Loveland, CO.), a bandsaw was used to cut the tibia to a desired length. A customized fixture was used to grip the patellar bone and a 2500 kg load cell was used to measure load on the tendon. After mounting the sample in the MTS machine, the tendon was pulled taut (1.5 kg) and two dark lines were applied by attaching monofilament suture material to the tendon with cyanoacrylate (Figure 5.2). A Visual Dimensional Analysis (VDA) (Living Systems Instrumentation, Burlington, VT) system was used to measure the visual change in strain between the dark lines.

The mechanical tests were conducted under load control with a preload of 15 N was applied to all of the tendons. They were then subjected to 10 cycles of preconditioning (ramp loading) from 5 N to 50 N at 10N/sec. Immediately after preconditioning, the patellar-tendon-tibia complex was pulled at a constant rate of 2.5 N/sec until the tendon reached the desired strain as indicated by visual monitoring of visual display on the VDA. The VDA was calibrated and used to monitor the percent change in strain in the tissue. The strain measurement

increased to 3%, 4%, or 6% of the tendon's initial measurements and the test was held. The tests were conducted in load control and as the tendon was held at the designated strain rate some creep may have occurred over time. While being held at their respective percent strains, the specimens were injected with 10 cc's of fixative solution (5 cc's given at 10 minute intervals). After 20 minutes, the tendon was detached with a scalpel; the central center piece was dissected and placed in a vial of fixative at 4ºC. While being tested, the tendon was continuously sprayed with a saline solution to retain moisture. Load, displacement, and VDA data was recorded via a local computer (Figure 5.1). The three channels were placed into the multiplexer and the data was then converted from analog to digital. The sampling rate was 2500 measurements per second and the data was obtained with Labview software (National Instruments, Austin, TX). The control sample was attached to the MTS system, a preload of 15 N was applied and the monofilament sutures were attached. The control samples were placed in the MTS for 10 minutes and they were not stretched further.

Visual Dimensional Analysis Setup and Calibration. A Hitachi camera was connected to the VDA system and used to view the tendon. The image received from the camera and to the VDA system was then displayed on the TV monitor. Two sutures were placed on the tissue to monitor change in strain and the strain change was measured in the center portion of the tendon. The VDA system was calibrated to track the displacement of the sutures. As the tendon was pulled, the strain increased and the area between the sutures ("diameter") increased.

For calibration purposes the area between the sutures was noted as the "diameter" and the left suture was noted as the "left wall" and the "right suture" was noted as the right wall. The wall and diameter calibration processes were separate. For calibrating the wall measurements the left and right windows on the VDA system was located and positioned by using the start and width controls. The "diameter" was calibrated similarly to the wall calibration and the "diameter" or area between the sutures was set to a known value and tracked with the VDA when testing began.

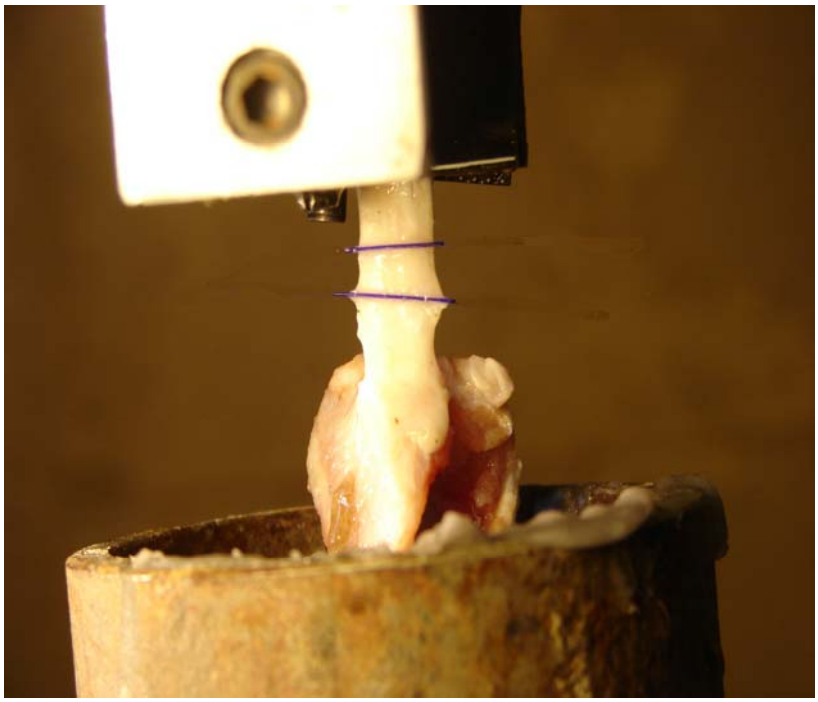

Figure 4.2

Tendon set up on MTS in preparation

Transmission Electron Microscopy. Immediately after the central center portion of the tissue was removed via sharp dissection with a scalpel, it was placed in a fixative solution in preparation for TEM. The patellar tendon tissue pieces were fixed in ½ strength Karnovsky's (in 0.1M cacodylate buffer, pH 7.2) and remained in the fixative solution for seven days in a 4ºC environment. The tendon specimens were rinsed in 0.1M sodium cacoldylate buffer (pH 7.2). After rinsing, they were fixed in 1% osmium tetra oxide (in 0.1M sodium cacoldylate buffer, pH 7.2) for two hours, and then placed in 1% (aqueous) tannic acid for 1 hour. Thereafter, they were placed in 1% osmium tetra oxide (in 0.1M sodium cacodylate buffer, pH 7.2) for two hours. The tissue underwent two buffer rinses and two water rinses and followed by dehydration in a graded ethanol series. The tissue was infiltrated and embedded in Spur's resin. Sections were cut perpendicular to the longitudinal axis at 75 nm thickness on a Reichert Jung Ultra cut E ultra microtome and viewed on a JEOL JEM 100CXII (JEOL USA, Peabody, MA.) transmission electron microscope at 60 kilovolts. Electron micrographs of 6 randomly selected equal sized fibril fields within the fascicles of each tendon segment were obtained (20,000 X magnification).

Image Analysis. The fibrils in each image were approximated as being circular in shape. The image areas were 4.5 x 3.1 μm^2 and there were between 283 and 401 fibrils per image. The digitized TEM images were analyzed using Image J Software (National Institutes of Health, Baltimore, MD). One image (n=1) of the control specimen was analyzed and then one image (n=1) at 3%,

one image (n=1) at 4% strain, and one image (n=1) at 6% strain were analyzed. A total of 4 images were processed and analyzed and the number density, area fraction and diameter distributions were determined from each image. The number density (ND) was calculated using equation 1, the area fraction of the fibrils was calculated by using equation 2, and mean fibril diameter was noted as the average size of the fibril diameters within each section. The number density units are fibrils per micrometer squared, area fraction denotes the percent fiber area within the area of the image analyzed, and the diameter distribution is demonstrated by histograms of frequency vs. diameter size, which is in nanometers. Please see the methodology in study 1 for additional details.

Results

Table 4.1.

Number density, area fraction and fibril diameter of rabbit patellar tendon under no strain and at 3,%, 4%, and 6% strain

Tendon Section	Number Density (fibrils/μ^2)	Area Fraction (%)	Mean Fibril Diameter (nm)
Control	27	54	150
3%	21	85	212
4%	22	86	210
6%	20	79	212

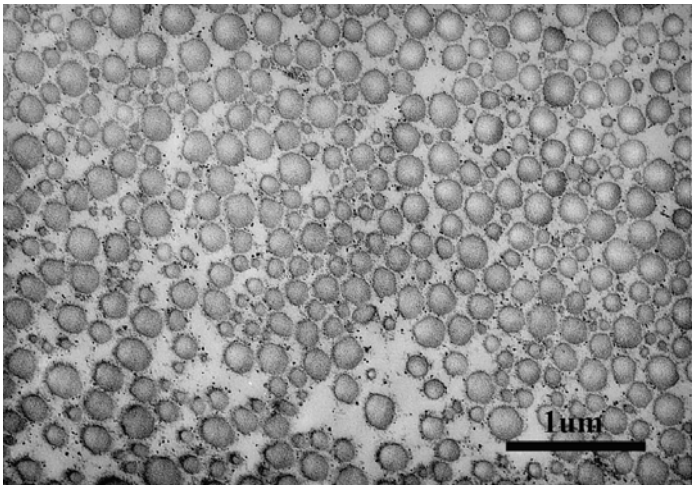

Figure 4.3

TEM image of the control tendon

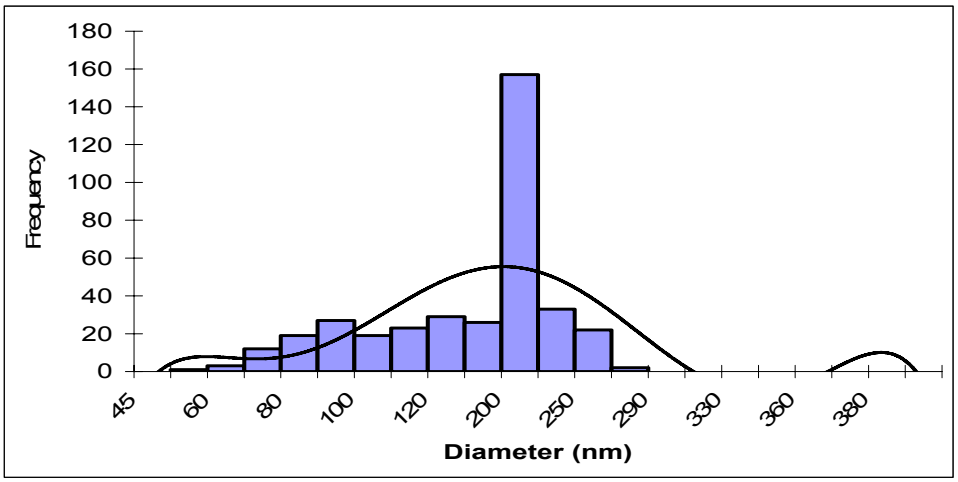

Figure 4.4

Diameter distribution of collagen fibrils within the control tendon

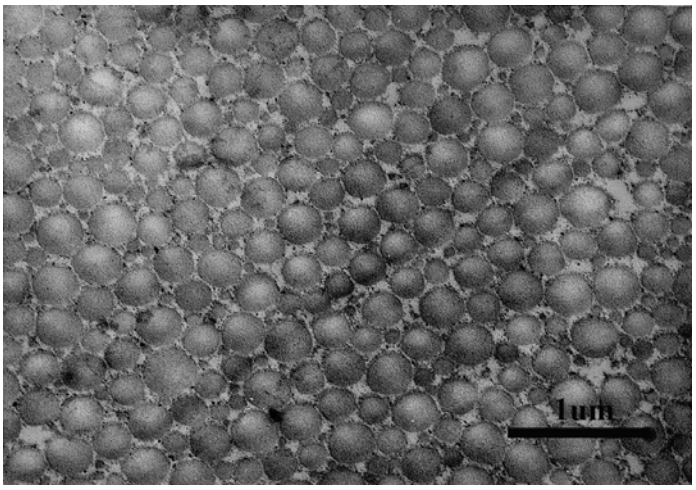

Figure 4.5

TEM image of the tendon pulled to 3 percent strain

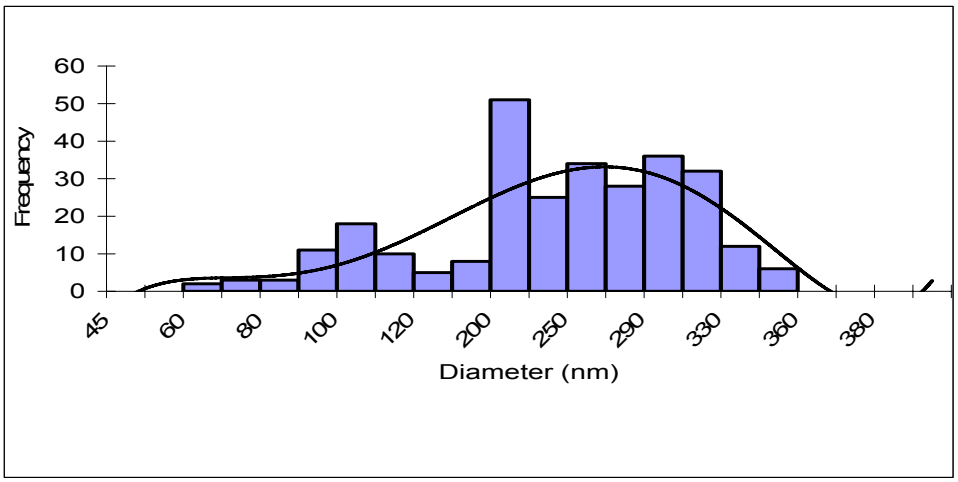

Figure 4.6

Diameter distribution of collagen fibrils within the tendon pulled to 3 percent strain

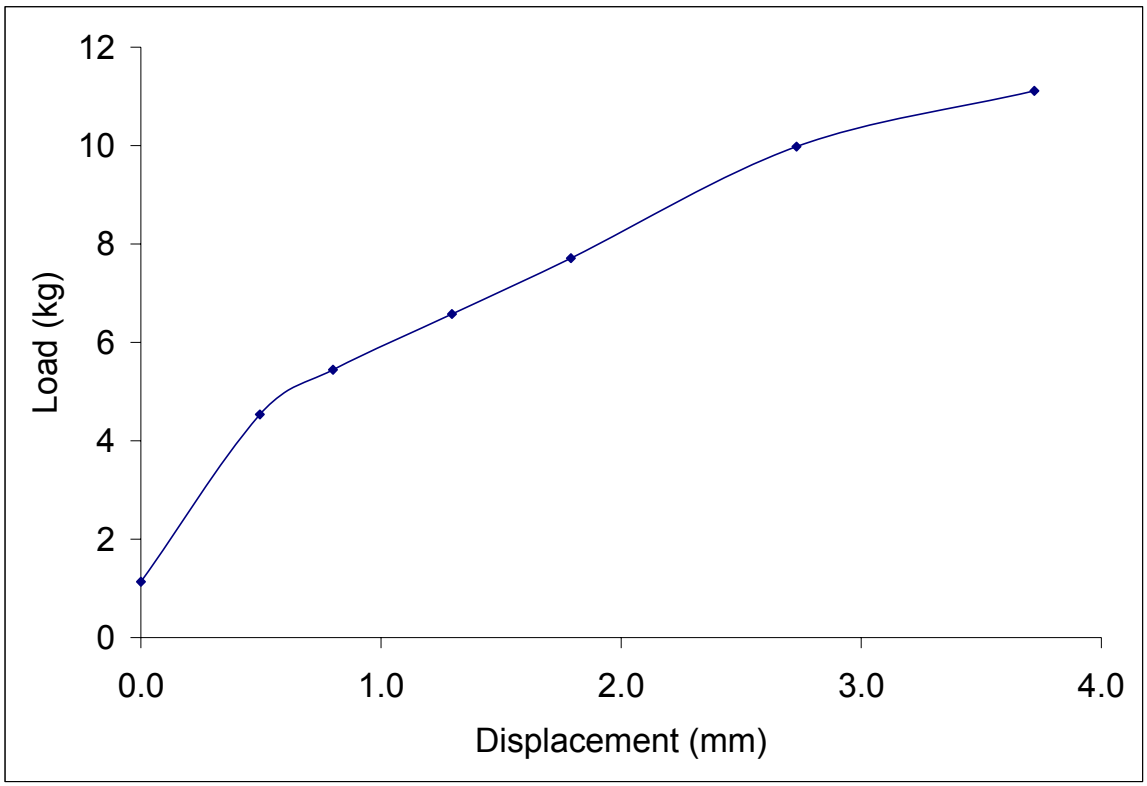

Figure 4.7

Load-displacement response of tendon pulled to 3 percent strain

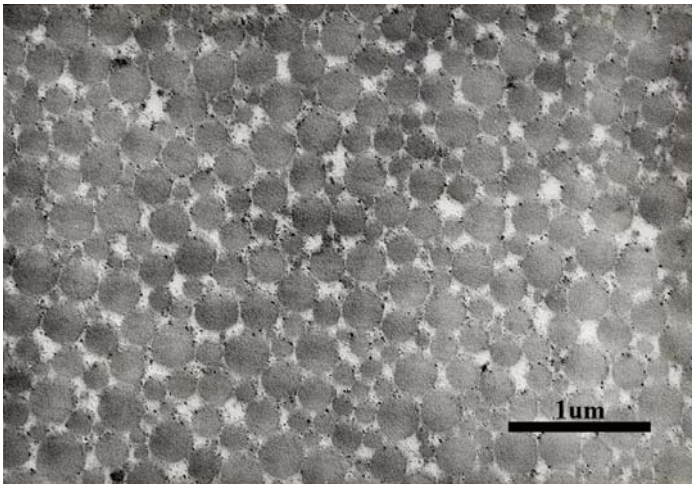

Figure 4.8

TEM image of the tendon pulled to 4 percent strain

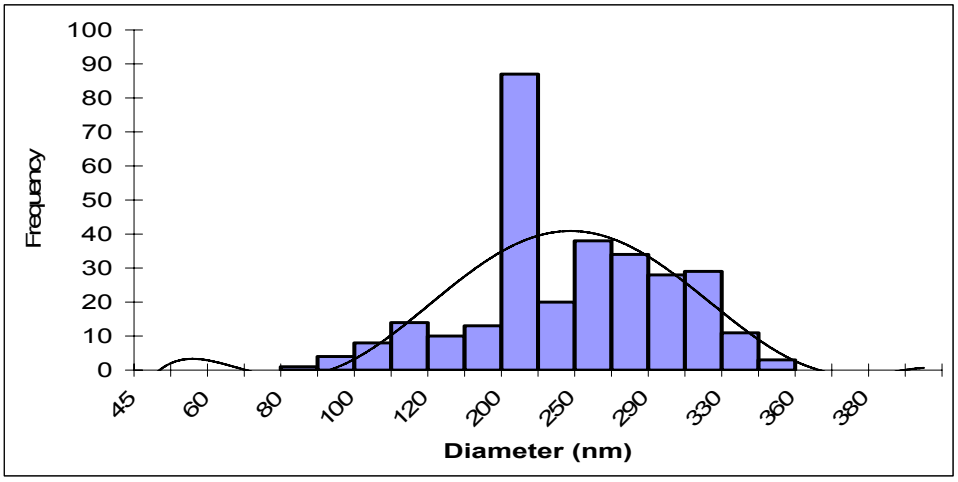

Figure 4.9

Diameter distribution of collagen fibrils within the tendon pulled to 4 percent strain

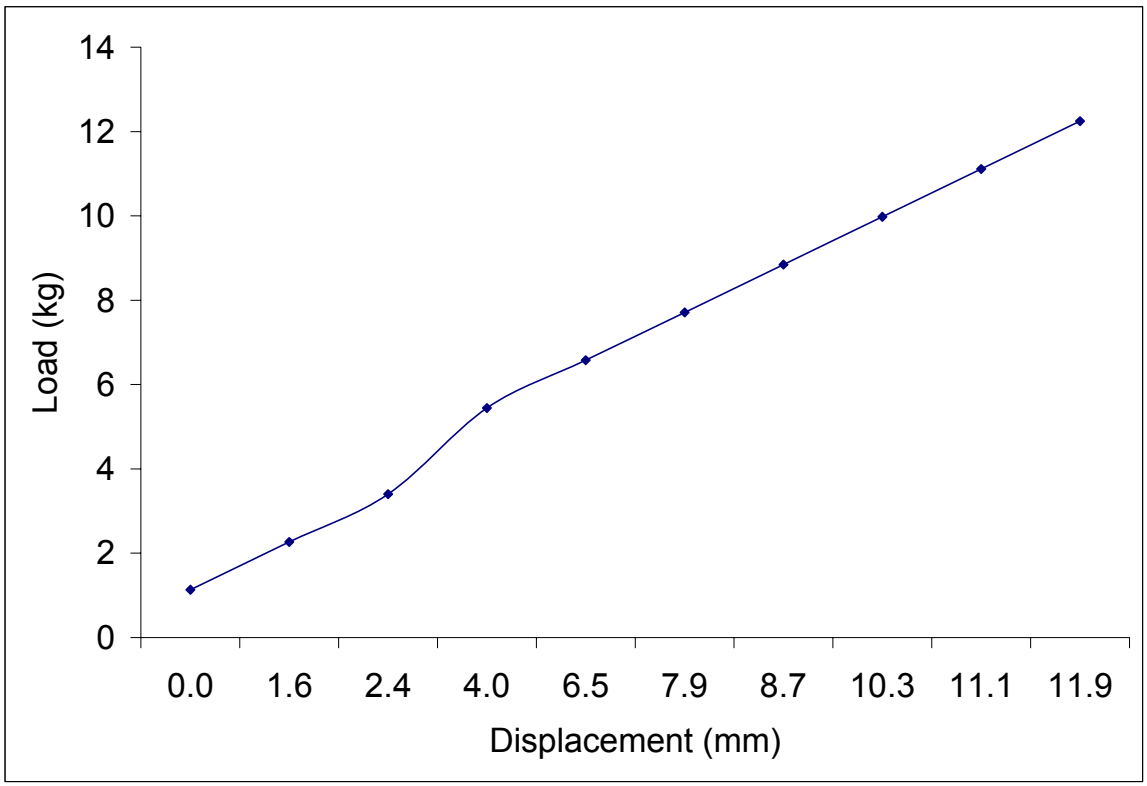

Figure 4.10

Load-displacement response of tendon pulled to 4 percent strain

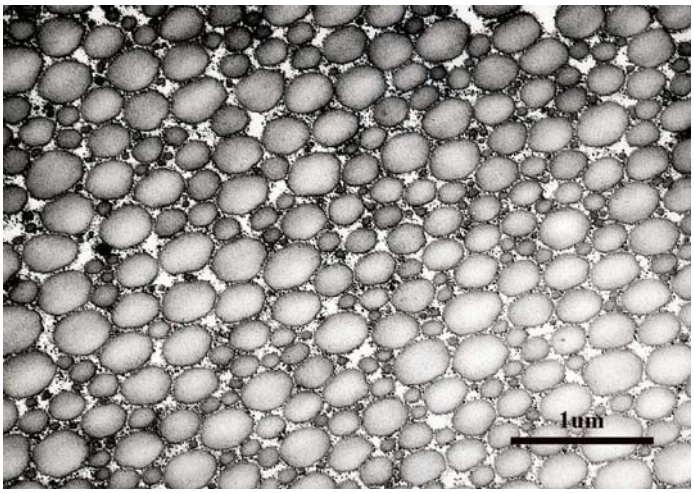

Figure 4.11

TEM image of the tendon pulled to 6 percent strain

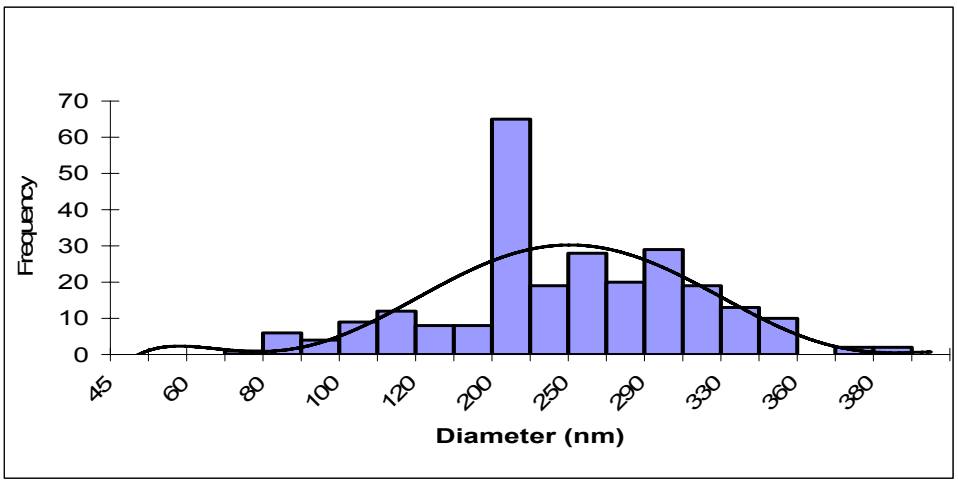

Figure 4.12

Diameter distribution of collagen fibrils within the tendon pulled to 6 percent strain

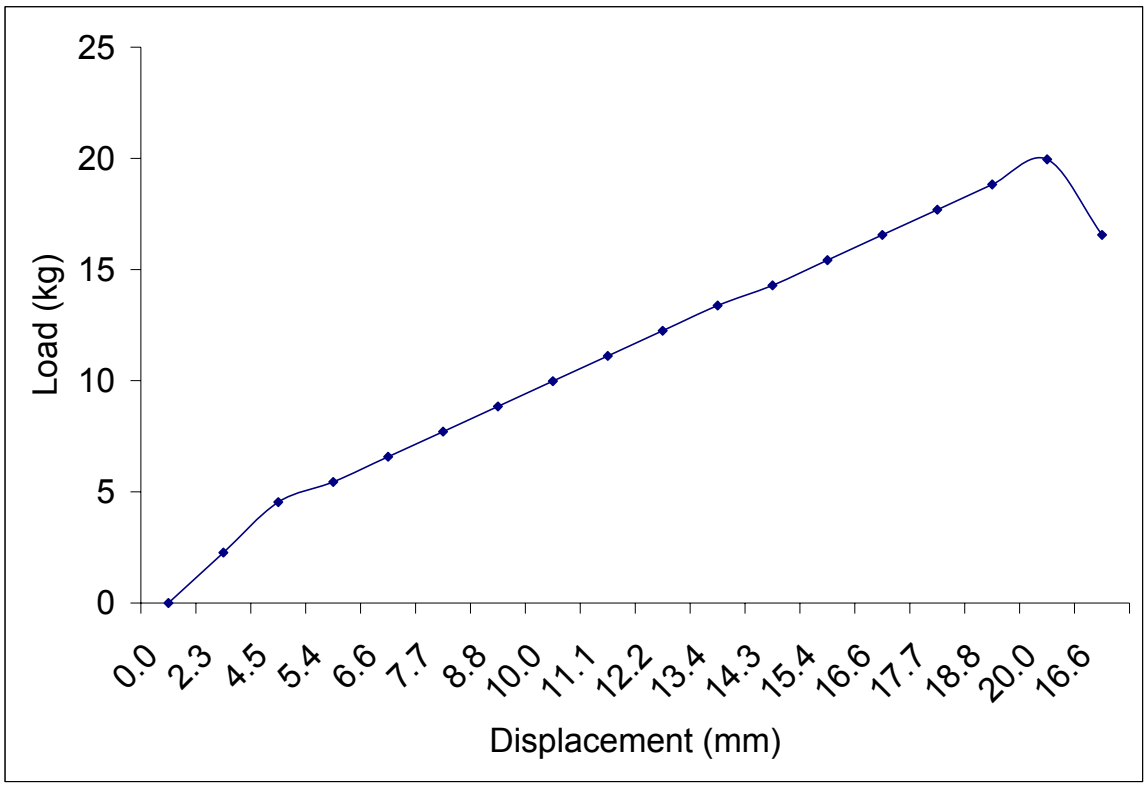

Figure 4.13

Load-displacement response of tendon pulled at 6 percent

Discussion and Conclusion

The results from this study are limited due to the fact that only one tendon was examined for each level of strain. However, it is evident that the control specimen exhibited a smaller mean diameter size and area fraction and larger number density. On the contrary, the 3%, 4% and 6% specimens had larger mean diameter sizes and area fraction and smaller number densities. Although not subjected to any load, the values for the samples in study 1 are much closer to the values of the pulled samples within this test and not the control. This is

one reason further testing is needed for examination of the effect of load on fibers.

Parry et al. (1977) and Binkley and Peat (1986) positively correlated changes in fibril diameter with changes in mechanical properties of the tendon. However, in Lavagnino's (2005) examination of rat tail tendon, the authors showed that fibril diameter was negatively correlated with the mechanical response and thus concluded that the diameter distribution did not, by itself, reflect changes in the tendon's mechanical response. Lavagnino's study implies that there are additional mechanisms, along with diameter distribution, that may affect mechanical behavior. The possible other mechanisms influencing mechanical behavior could be proteoglycans binding at adjacent fibers to assist in force transfer, collagen crosslinking, length of the collagen fibril , and cellular mechanics. Mechanical environment changes are sensed by the cells, which alter GAG and PG synthesis (Akeson et al. 1973). GAGs and PGs play a major role in stress transfer through the fiber to the tendon and they also regulate collagen fibrillogenesis and therefore will ultimately adapt the fibril distribution to the tissue's new mechanical requirements. There have been many investigations on the mechanical effects of increasing collagen crosslinking (Thompson et al. 1995 and Haut 1985). The results of increased crosslinking of collagen demonstrated an inhibition of collagenase activity which may ultimately lead to a reduction in the strain to failure of collagen and an increase in its tensile modulus. This "stiffening" makes the material appear more brittle and less

ductile and possibly causing early fracture. If the length of the collagen fibril is greater than some critical value, then the fibril will be able to act as a high tensile element and ultimately change the mechanical behavior of the overall material. Parry (1988) presents an expression for determining the critical length (Lc) that is written as follows:

$$Lc = \frac{(RadiusOfCollagenFibril * TheBreakingStressOfThatFibril)}{ShearStressExertedOnTheFibrilByMatrix} \quad (6)$$

This equation shows that the critical length has a positive correlation with the fibril diameter and therefore causes an increase in tensile attributes. The shear stress depends on the interactions between the collagen fibrils and the GAGs constituting the matrix. As the interactions increase, the shear stress exerted on the matrix will increase and create greater tensile attributes. The need for a higher critical length will be less because of compensation from the shear stress. Cellular mechanics are also important in the examination of mechanical integrity of the tendon. Arnoczky (2002) used confocal microscopy to examine the in situ response of cells of the tendon while under varying magnitudes of strain (0%, 2%, 4% and 6%). The results of this study indicated that application of a tensile load to a tendon results in an in situ deformation of the cell nuclei. This nuclear deformation may affect the overall cell signaling process because others have noted that the cellular membrane mechanical deformations are transduced into an intracellular signal through cytoskeletally mediated nucleus deformation

(Banes et al. 1995; Guilak 1995). The overall result of nuclear deformation could possibly be a result of cellular membrane deformation.

The aforementioned aspects may be contributors to the outcome of the results of this study. The graphical results show that the tendons are unimodal although the TEM images of the pulled specimens visually appear bimodal. Study 1 within this dissertation shows most of the central sections as having a bimodal distribution. Parry (1978) showed that the division between tissues showing unimodal or bimodal fibril distributions at maturity does not simply relate to the type I collagen/type II collagen classification, or directly to the levels of stress and strain encountered by the tissue. Reasoning being because skin has an ultimate tensile strength between that of cartilage and tendon modulus and the fibril distribution in skin is primarily unimodal while the fibril distribution of cartilage and tendon is bimodal. Although, Parry does state that there appears to be a relationship between bimodality and maturity along with the tissue maintaining stresses over a long period of time. Zhang et al. 2005 also showed that tendon fibril diameter increased with maturity. Parry (1977) stated that the doublet or triplet conjoined fibers are usually seen in fibers of tendons that are stretched at 3% or less strain. Doublet conjoined fibers are two fibers that appear to merge together to form 1 fiber and triplet conjoined fibers are three fibers that merge together to form 1 fiber. This conjoining phenomenon was not observed in the control or 3% specimens, which were both subjected to strains of 3% or less.

When the tendon is stretched instantaneously the physiological processes in the tissue are activated. The magnitude of tissue strains may cause variation in the response. As noticed in Figures 4.7, 4.10, and 4.13 the load required to reach each respective percent strain increased as the desired strain increased. As for the 6% tendon, the collagen fibers began to rupture after being subjected to 6% strain. The tissue is undergoing internal changes while being subjected to such loads. Fluid exudation and water volume loss occur during uniaxial loading of the tendon. These two phenomena account for the fiber-aligned Poisson's ratio of the tendon to be near a value of 3. Also, the PGS within the tendon are highly negative charged molecules that have the ability to catch an amount of water which is 50 times their weight. During stress on the tendon the PGs are compressed approximately 20 percent, which contributes to water exudation from the tendon. Water, which comprises much of the tendon matrix, along with the PG's and GAGS contributes to the high viscoelastic properties of the tendon. Viscoelasticity allows the tendon to absorb high stresses and recover when subjected to extended periods of rest. As the strains increase on the tendon, more water exudes which lengthens its recovery time and may cause damage or failure if the stresses are exceedingly high. The water binding capacity of the macromolecules improves the elasticity of the tendon. When the water leaves the tendon and the stiffly extended PG bonds begin to break the fibril strength becomes compromised and ultimate failure occurs. PG's enable rapid diffusion of water soluble molecules and assist with migration of cells and they also

stabilize the system of connective tissue. If cell migration is not possible in the tendon due to limited PG activity then mechanotransduction will be limited and this will also contribute to the lack of the tendon's ability to maintain high stresses. It is likely that mechanotransduction, in response to tissue load, is mediated through extracellular matrix deformation. Arnoczky (2002) showed that the differential tissue strains may exist in the same local area of a stressed tendon is a unique structural characteristic that results in a pattern of in vivo cell deformation and allow recruitment of specific cells at each level of tissue strain. However, as previously mentioned, excessive strains may alter this deformation pattern and result in over or under expression of cell responses. Therefore, the 6% strain specimen could have failed due to either of the aforementioned phenomena. PGs stiffness and cell migration was possibly more active in the 3% and 4% tendons and therefore failure did not occur.

More insight is required on this study for definitive results to be concluded. Future work includes analyzing additional images of each treatment to obtain an average diameter distribution, number density and area fraction based on the specific treatments. Additional testing on more tendons will also be performed along with TEM studies. The stress-strain curves will be evaluated and compared between the control tendons and the tendons subjected to load. The fibrils of the samples pulled at 6% were slightly elongated in Figure 4.11 and therefore the diameter distribution may be slightly skewed because the fibrils were assumed to be circular in the analysis. Additional images analyzed from

this section will decrease the error. Another consideration is that the tests in this study were under load control and at the end of the test as the specimens were being fixed load was held constant, which may have allowed creep to occur and slightly change the true load response of each tendon. Future tests should possibly be conducted under displacement control. Also, an evaluation of the relationship of PGs and GAGs of pulled tendons should be examined to confirm their response as the tissues is being pulled.

References

[1] An KN (2005) Role of biomechanics in functional tissue engineering. In:Mechanical properties of bioinspires and biological materials. (ed) Viney C, Katti K, Ulm FJ and Hellmich C. Materials Research Society, Warrendale

[2] Akeson W, Woo S, Amiel D, Couts R and Daniel D (1973) The connective tissue response to immobility: biochemical changes in periarticular connective tissue of the immobilized rabbit knee. Clinical Orthopedics and Related Research 93:356-362

[3] Arnoczky S, Lavagnino M, Whallon J and Hoonjan A (2002) In situ cell nucleus deformation in tendons under tensile load; a morphological analysis using confocal laser microscopy. Journal of Orthopedic Research 20:29-35

[4] Banes A, Tsuzaki M, Yamamoto J, Fischer T, Brigman B, Brown T and Miller L (1995) Mechanoreception at the cellular level the detection interpretation, and diversity of responses to mechanical signals. Biochemistry and Cell Biology 73:349-365

[5] Binkley J and Peat M (1986) The effect of immobilization on the ultrastructure and mechanical properties of the medial collateral ligaments in rats. Clinical Orthopaedics and Related Research 203:301-308

[6] Derwin K and Soslowsky L (1999) A quantitative Investigation of structure – function relationships in a tendon fascicle model. Journal of Biomechanics 121:598-604

[7] Elliott D (1965) Structure and function of the mammalian tendon. Biological Reviews 40:392-421

[8] Guilak F (1995) Compression-induced changes in the shape and volume of the chondrocyte nucleus Journal Biomechanics 28:1529-154

[9] Hannafin J A and Arnoczky S P (1994) Effect of cyclic and static tensile loading on water content and solute diffusion in canine flexor tendons: An *in vitro* study. Journal of Orthopedic Research 12:350-356

[10] Haut R (1985) The effect of a lathyritic diet on the sensitivity of tendon to strain rate. Journal of Biomechanical Engineering 107:166-174

[11] Kastelic J, Galeski A and Baer E (1978) The multicomposite structure of tendon.ConnectiveTissueResearch6:11-23

[12] Lavagnino, M, Arnoczky, S, Frank, K and Tian, T (2005) Collagen fibril diameter distribution does not reflect changes in the mechanical properties of in vitro stress-deprived tendons. Journal of Biomechanics 38:69-75

[13] Lynch H A, Johannesen W, Wu J P, Jawa A and Elliott D (2003) Effect of fiber orientation and strain rate on the nonlinear uniaxial tensile material properties of tendon. Journal of Biomechanical Engineering 125: Parry D and Craig A (1977) Quantitative electron microscope observations of the collagen fibrils in rat-tail tendon. Biopolymers 16:1015-1031

[14] Parry, D, Barnes, G and Craig, A (1978) A comparison of the size distribution of collagen fibrils in connective tissue as a functiion of age and a possible relation between fibril size distribution and mechanical properties. Proceeding of the Royal Society of London B 203:305-321

[15] Parry DA (1988) The molecular and fibrillar structure of collagen and its relationship to the mechanical properties of connective tissue. Biophysical Chemistry 29:195-209

[16] Rigby B, Hirai N, Spikes J and Eyring H (1958) The mechanical properties of rat tail tendon. The Journal of General Physiology 43: 265-283

[17] Robinson PS, Lin TW, Jawad AF, Iozzo RV and Soslowski LJ (2004) Investigating tendon fascicle structure-function relationships in a transgenic age mouse model using multiple regression models. Annals of Biomedical Engineering 32:924-931

[18] Sasaki N and Odajima S (1996) Elongation of collagen fibrils and force-strain relations of tendons at each level of structural hierarchy. Journal of Biomechanics:1131-1136

[19] Thompson J and Czernuszka J (1995) The effect of two types of cross-linking on some mechanical properties of collagen. Bio-Medical Materials and Engineering 5:37-48

[20] Toyhama H and Yasuda K (2002) The effect of increased stress on the patellar tendon. Journal of Bone and Joint Surgery (Br) 84:440-446

[21] Viidik A (1980) Mechanical properties of parallel-fibered collagenous tissues. In:Biology of Collagen. (ed) A Viidik and J Vuust. Academic Press, London

[22] Woo S, Livesay G, Runco T and Young E (1997) Structure and function of ligaments and tendons. In:Basic Orthopaedic Biomechanics. (ed) Mow V and Hayes W Lippincott-Raven, Philadelphia

[23] Yamamoto E , Hayashi K, Kuriyama H, Ohno K, Yasuda K and Kaneda K (1992) Mechanical properties of the rabbit patellar tendon. Journal of Biomechanical Engineering 114:332-337

[24] Zhang G, Young B, Ezura Y, Favata M, Soslowski L, Chakravarti S and Birk D (2005) Development of tendon structure and function: Regulation of collagen fibrillogenesis. Journal of Musculoskeletal and Neuronal Interactions 2005:5-21

CHAPTER V

APPLICATION OF TESTING: MULTIAXIAL STRESS STATES AND CONCLUSIONS

The large deformation mechanical response in tendons is a function of the material substructure. Bull (1957) explained the tendon's configuration as that of a nylon thread and fabric. The thread is stiff and the fabric stretches easily within the direction of tension. The stress-strain response of the thread is steep and rather linear with a small amount of hysteresis, while the response of the fabric is nonlinear with a toe region of the curve. However, unlike the thread and fabric combination, the tendon's components interact with macromolecules, such as glycoproteins and other cellular components that contribute to the variation of stress-strain responses based on each state of stress to which the tissue is subjected. From a kinematics aspect, soft tissues will not respond the same as that of materials that are not viscoelastic or do not have a time dependent response. The deformation gradient, *F,* is commonly decomposed into elastic and plastic parts. Inelastic parts, which may represent volume change, also have been placed in *F*. However, before including these terms into a continuum framework, the phenomena of the material must be known and understood.

The viscoelastic a phenomenon in tissues is attributed to many aspects, as previously mentioned; therefore quantification of the time dependent aspect within the deformation gradient has not been extensively developed. As the tissue is subjected to either of the 3 major stress states, tension, compression, or simple shear, the dissipative responses will vary between the stress states. This will ultimately cause variation in the stress strain responses.

Figures 5.1 and 5.2 represent the stress-strain responses (in von Mises stress space) of the rabbit patellar tendon. Figure 5.1 displays the responses of the tendon in transverse orientation while being subjected to tension, compression, or simple shear at 0.001/s. Figure 5.2 displays the responses of the tendon in the longitudinal orientation while being subjected to tension, compression or simple shear at 0.001/s. For both testing orientations, the tendon in tension experienced higher stresses at the same strains, the stresses decreased with shear testing and under compression the tendon displayed the smallest stresses.

The tensile responses demonstrated greater stresses than both the simple shear and compressive loading. The phenomenon behind the high tensile strength is the strength of the parallel collagen fibers, which stabilizes the structure. Interactions among fibrous components, specifically the lateral covalent crosslinks, have been attributed to the added strength within the linear regions of the viscoelastic structures. The shear responses demonstrate the second highest stresses. In areas of compression, specifically where

fibrocartilaginous matrices are formed, the tissue experiences shear forces. One of the distinguishing characteristics of fibrocartilage is the collagen fibers running at angles to one another, or shearing (Vogel 2003). Also, tendon matrix-fiber interactions are also responsible for increased shear stresses. This shearing magnitude is highly dependent on the interactions between the collagen fibrils and the hydrated glycosaminoglycans within the matrix. The compressive response demonstrated the smallest stresses, which are likely due to buckling of the fibers. Although the tendon underwent compressive loads, fibrocartilage was not evident on the tendon, thus it is not likely to play a role in the tendon's response to compression.

In terms of modeling, the stress state dependency will be a function of an internal damage parameter within the model. The constants needed to incorporate into the model to account for tension, compression, and simple shear will be determined via experimentation. The future model also will be a function of the effective or von Mises stresses, as this will denote stress state dependency within the model and allow mapping of shear and uniaxial stresses. The advantage of von Mises criterion is its ability to fit experimental data better than other theories because no knowledge is needed regarding the relative magnitudes of the principal stresses. In order to incorporate the underlying physics into the ISV model, kinetics equations (flow rule) will be developed. The flow rule is a function of the von Mises stress state and the inversion of the flow rule is the von Mises yield.

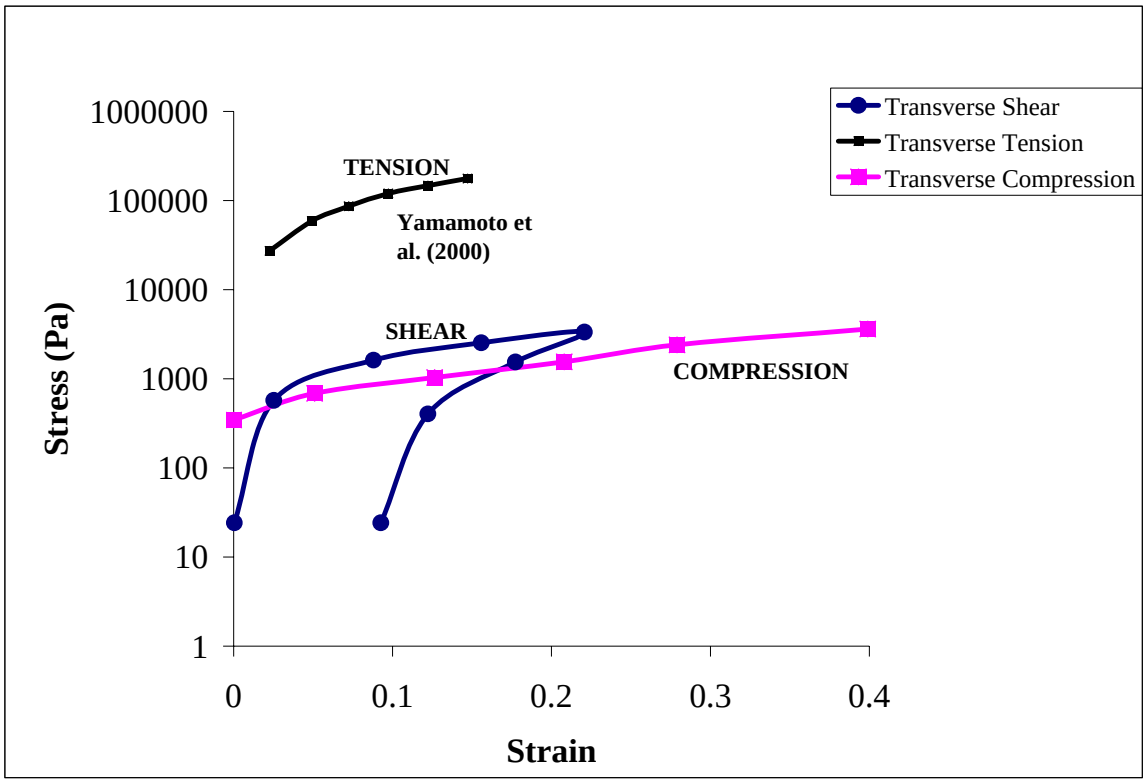

Figure 5.1

Von Mises Stress Strain Curve of Tendon—Transverse Loading at 0.001/s

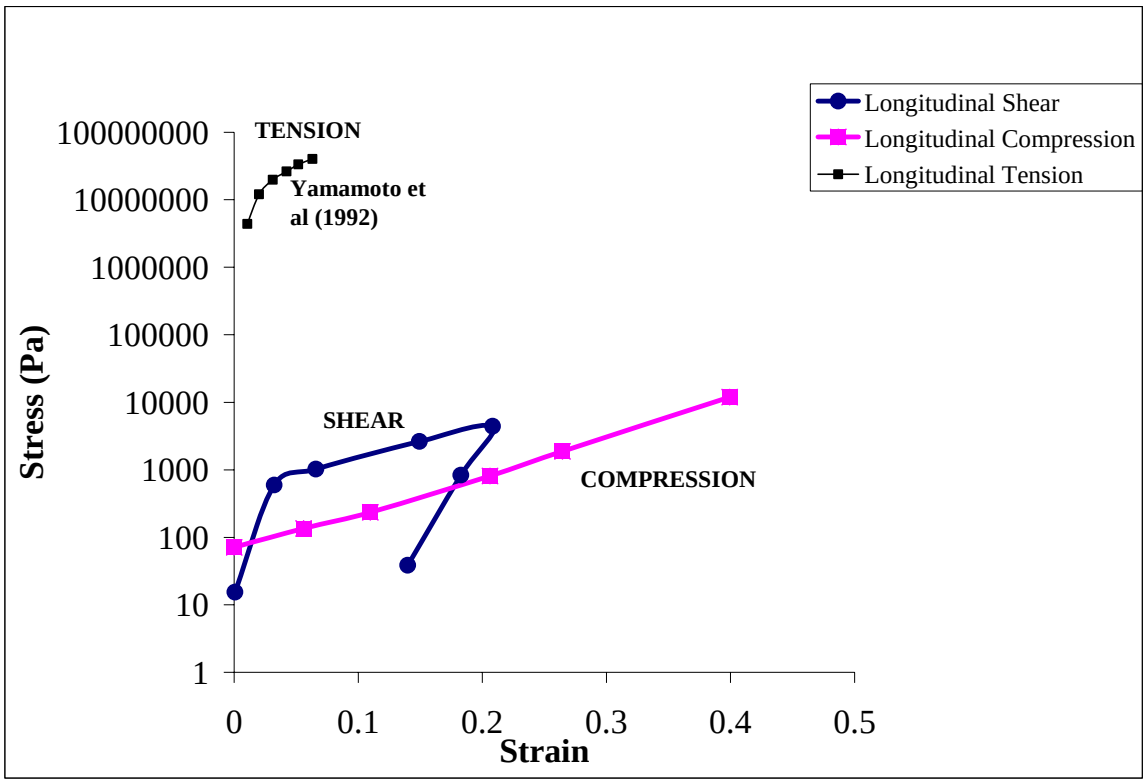

Figure 5.2

Von Mises Stress Strain Curve of Tendon—Longitudinal Loading at 0.001/s

Conclusions

The overall results of this dissertation show variability within the structural fibril network along with the compressive anisotropy within the rabbit patellar tendon. Table 5.1 shows the contributions of this dissertation to fill in the missing links for model development. The compression study in this dissertation has now contributed to the ability to formulate the anisotropic stress-strain responses of the rabbit patellar tendon. It has been assumed that the rabbit patellar tendon is anisotropic however; there has not been any data to secure that hypothesis. Now, we have contributed to the fact of compressive anisotropy within the rabbit patellar tendon. Also, this study contributes to the macroscale stress state information on the rabbit patellar tendon, which will later be incorporated into a stress state independent model. The tension quantified TEM data shows a unique trend for the pulled specimens. Further investigation is required to gather statistically significant results. The structural data in this study will contribute to further development of the Internal State Variable model.

Table 5.1

Contributions to experimental research required for model development

	TENDON		FASCICLE		FIBRIL	
	Longitudinal	Trans-verse	Longitudinal	Trans-verse	Longitudinal	Trans-verse
TENSION	A (Yamamoto et al. 1992)	A (Yamamoto et. al, 2000)	NOT (Yamamoto et al. 1999)	NOT	NOT	NOT
COMPRESSION	*A*	*A*	NOT	NOT	NOT	NOT
SIMPLE SHEAR	A Our group	A Our group	NOT	NOT	NOT	NOT
INDENTER	n/a	NOT	NOT	NOT	NOT	NOT
VOLUMETRIC FRACTION	n/a		NOT		*A*	
Key:	A denotes Availability				NOT denotes limited to No Availability	

Although this study has contributed information to the development of the viscoelastic material model, Table 5.1 shows that an extensive amount of work must be completed to gather model parameters. Future studies will include examinations of the mechanical properties of the tendon at lower length scales. Specifically, mechanical testing at the fibril and fascicle level of the tendon is

required for microstructural information to input for model exploration. Considering that internal state variables account for damage due to internal processes, it would be feasible to study the tendon at the atomistic level and examine macromolecules and cellular response based on stress states. A detailed study into the effects of proteoglycans and glycosaminoglycans should occur to also incorporate their effects into the development of the ISV model. Investigations of finite element analysis of compression in both the longitudinal and transverse orientation should be performed to verify our experimentation. The tendon was subjected to both a distributed load and a point load during compression testing, to understand the stress distribution a viscoelastic simulation of the tendon should be performed to simulate the testing protocol. Viscosity and fluid flow parameters for the tendon are also required for the model development. After the model has been completely developed, testing should be performed to validate the developed model. Specifically, if the tendon is subjected to multiple stress states in one test cycle and the stress-strain response is recorded, the model should be able to predict the response of the tendon.

References

[1] Bull, H (1957) Protein structure and elasticity. In:Tissue Elasticity. (ed) Remington, J. American Physiological Society.

[2] Vogel, K (2003) Tendon structure and response to changing mechanical load. Journal of Musculoskeletal Neuron Interaction 3:323-325

APPENDIX A

DIAMETER DISTRIBUTION ANALYSIS OF VARIANCE

Table A.1

Pairwise Comparisons of Mean Stiffnesses

Dependent Variable: MEAN

(I) SECTION	(J) SECTION	Mean Difference (I-J)	Std. Error	Sig.(a)	95% Confidence Interval for Difference(a) Lower Bound	Upper Bound
Size1	Size2	23.000	18.099	.240	-18.737	64.737
	Size3	46.000	20.522	.055	-1.325	93.325
	Size4	-17.000	20.522	.431	-64.325	30.325
	Size6	38.500	20.522	.098	-8.825	85.825
Size2	Size1	-23.000	18.099	.240	-64.737	18.737
	Size3	23.000	21.633	.319	-26.885	72.885
	Size4	-40.000	21.633	.102	-89.885	9.885
	Size6	15.500	21.633	.494	-34.385	65.385
Size3	Size1	-46.000	20.522	.055	-93.325	1.325
	Size2	-23.000	21.633	.319	-72.885	26.885
	Size4	-63.000(*)	23.697	.029	-117.646	-8.354
	Size6	-7.500	23.697	.760	-62.146	47.146
Size4	Size1	17.000	20.522	.431	-30.325	64.325
	Size2	40.000	21.633	.102	-9.885	89.885
	Size3	63.000(*)	23.697	.029	8.354	117.646
	Size6	55.500(*)	23.697	.047	.854	110.146
Size6	Size1	-38.500	20.522	.098	-85.825	8.825
	Size2	-15.500	21.633	.494	-65.385	34.385
	Size3	7.500	23.697	.760	-47.146	62.146
	Size4	-55.500(*)	23.697	.047	-110.146	-.854

Based on estimated marginal means

* The mean difference is significant at the .05 level.

a Adjustment for multiple comparisons: Least Significant Difference (equivalent to no adjustments)